# Colloidal size spectra, composition and estuarine mixing behavior of DOM in river and estuarine waters of the northern Gulf of Mexico

Zhengzhen Zhou[a,b], Björn Stolpe[a,c], Laodong Guo[a,b]* and Alan Shiller[a]

a) Department of Marine Science, University of Southern Mississippi, Stennis Space Center, MS 39529, USA
b) School of Freshwater Sciences, University of Wisconsin-Milwaukee, 600 East Greenfield Avenue, Milwaukee, WI 53204, USA
c) Akzo Nobel Pulp & Performance Chemicals, 445 80 Bohus, Sweden

*Corresponding author. Tel: 414-382-1742; e-mail: guol@uwm.edu.

*GCA*

**Abstract**

Flow field-flow fractionation (FlFFF) coupled on-line with UV absorbance and fluorescence detectors was used to examine the colloidal composition and size distribution of optically active dissolved organic matter (DOM) in the lower Mississippi River (MR), the East Pearl River (EPR), the St. Louis Bay (SLB) estuary, and coastal waters of the northern Gulf of Mexico. In addition to field studies, laboratory mixing experiments using river and seawater end-members were carried out to study the processes controlling the estuarine mixing behavior and size partitioning of colloids with different sizes and composition. The colloidal size spectra of chromophoric DOM and humic-like DOM showed one dominant peak in the 0.5-4 nm size range, representing >75% of the total FlFFF-recoverable colloids. In contrast, protein-like DOM showed a bi-modal distribution with peaks at 0.5-4 nm and 4-8 nm, as well as a major portion (from ~41% in the EPR to ~72% in the Mississippi Bight) partitioned to the >20 nm size fraction. Bulk DOM was lower in abundance and molecular-weight in the MR compared with the EPR, while the proportion of colloidal protein-like DOM in the >20 nm size range was slightly larger in the MR compared with the EPR. These features are consistent with differences in land use, hydrological conditions, and water residence time between the two river basins, with more autochthonous DOM in MR waters. In the SLB estuary, different DOM components demonstrated different mixing behaviors. The abundance of colloidal chromophoric DOM decreased with increasing salinity and showed evident removal during estuarine mixing even though the bulk DOM appeared to be conservative. In contrast, colloidal humic-like DOM behaved conservatively inside SLB and during laboratory mixing experiments. The ratio of colloidal protein- to humic-like DOM generally increased with increasing salinity, consistent with increasing autochthonous protein-like DOM and removal of terrestrially-derived humic-like DOM in estuarine and coastal waters. Similar mixing behavior for the bulk DOM and colloids was observed in short-term laboratory mixing experiments, suggesting that physicochemical processes are the major controlling factor for colloidal removal in the estuary. For the first time, this study showed direct evidence of contrasting estuarine mixing behavior for different size fractions of optically active colloidal DOM.

Keywords: Dissolved organic carbon, colloidal organic matter, flow field-flow fractionation, river waters, estuarine mixing

## 1. Introduction

Dissolved organic matter (DOM) is a major component of the global carbon cycle and plays an important role in regulating the biogeochemical cycling of nutrients and trace elements in aquatic systems (HEDGES, 2002; AIKEN et al., 2011; BAUER et al., 2013). The bulk DOM has been shown to be heterogeneous in size, composition, and chemical reactivity (GUO et al., 1996;HANSELL, 2013; BENNER and AMON, 2015). Among various sizes of DOM components, bulk DOM is composed of mostly colloidal organic matter or high-molecular-weight (HMW) DOM, especially in freshwater and estuarine environments (GUO and SANTSCHI, 2007; CAI and GUO, 2009).

Colloidal organic matter, operationally defined as the >1 kDa fraction of DOM (GUO and SANTSCHI, 2007), has been found to contain a variety of compounds and act as a dynamic intermediary between dissolved and particulate phases and regulates the transfer of some reactive metal ions to particles (HONEYMAN and SANTSCHI, 1989; GUO and SANTSCHI, 1997a). It also plays a critical role in regulating the concentration and speciation, and hence the fate, transport and bioavailability of trace metals and pollutants in aquatic systems (BENEDETTI et al., 2003; LEAD and WILKINSON, 2006; AIKEN et al., 2011; PHILIPPE and SCHAUMANN, 2014). The size of colloidal DOM determines its utilization efficiency by microbes (AMON and BENNER, 1996). Nevertheless, knowledge of the composition and size partitioning of colloidal DOM remains scarce, even though it should provide insights into the biogeochemical cycling pathways of DOM and trace elements in aquatic environments (STOLPE et al., 2010; STOLPE et al., 2013; PHILIPPE and SCHAUMANN, 2014).

Flow field-flow fractionation (FlFFF) is a chromatography-like technique in which the retention force is provided by a cross-flow perpendicular to the channel-flow, and colloids are separated based on their diffusion coefficients (GIDDINGS, 1993). A variety of detection systems, such as UV-absorbance and fluorescence, have been coupled online with FlFFF to examine the continuous colloidal size spectra of natural organic matter (ZANARDI-LAMARDO et al., 2002; STOLPE et al., 2010; GUÉGUEN and CUSS, 2011). Although applications of FlFFF to the investigation of the size distribution of natural DOM and nanoparticles in aquatic systems have been increasing (e.g., BAALOUSHA et al., 2011; Zhou and Guo, 2015), studies focusing on dynamic variability of colloidal organic matter during estuarine mixing are still few.

Estuaries are a dynamic aquatic environment where river water meets seawater and where changes in salinity, pH, turbidity, and DOM sources are the most dramatic (BIANCHI, 2007). Many previous studies have investigated the mixing behavior of bulk dissolved organic carbon (DOC) in different estuaries, including the St. Louis Bay estuary (Mississippi), showing both conservative and non-conservative mixing behavior (e.g., SHOLKOVITZ, 1976; MANTOURA and WOODWARD, 1983; GUO et al., 1999; WANG et al., 2010). Wang et al (2010) also showed that carbohydrate DOM components could be preferentially removed during estuarine mixing although the bulk DOC was somewhat conservative. It is likely that different sized colloidal DOM components may also behave differently during estuarine mixing due to their differences in composition and reactivity. Unfortunately, the estuarine mixing behavior of colloids with different sizes and composition remains poorly understood. Approaches combining both field studies and laboratory mixing experiments and using techniques capable of continuum separation and characterization of colloids are needed.

Our FlFFF system was coupled with both UV absorbance and fluorescence detectors targeting the chromophoric, humic-like and protein-like DOM components. Size spectra of colloidal DOM and their variations were examined and compared between two rivers, the lower Mississippi River (MR), a large river with a massive drainage basin and extensive anthropogenic influence (BECKETT and PENNINGTON, 1986; WIENER et al., 1996), and the Lower Pearl River (PR), a small black-water river that is less anthropogenically impacted (DUAN et al., 2007a; DUAN et al., 2007b). In addition, DOM composition and size spectra were determined in samples from the St. Louis Bay (SLB) estuary; the Mississippi Sound (MS), a nearshore water body that receives influence from the PR; and the Mississippi Bight (MB), a coastal water influenced by the MR, in the northern Gulf of Mexico. Furthermore, laboratory mixing experiments mimicking the estuarine mixing process were carried out and compared with the field results, in order to examine the estuarine mixing behavior of colloids with different sizes and composition.. Our study provides insights into how the abundance and size distribution of different types of colloids are influenced by hydrological conditions and land use in river basins, and what major biogeochemical processes and mechanisms control size distribution and mixing behavior of colloidal DOM in estuarine environments.

## 2. Materials and Methods

115 2.1. Study sites

116 The Mississippi River (MR), with an average flow rate of 17,000 $m^3/s$ and a drainage basin
117 covering about 40% of the contiguous United States (~3,220,000 $km^2$), is the fourth longest
118 (3,770 km) river in the world. Cropland covers about 58% of its drainage basin (GOOLSBY et al.,
119 2000; GOOLSBY and BATTAGLIN, 2001), and the river is largely constrained by dam systems and
120 levees (KEOWN et al., 1986; MEADE et al., 1990). Decreased suspended sediment and increased
121 nutrients, organic contaminants and trace elements in the recent past have caused eutrophication,
122 hypoxia and other environmental issues in the northern Gulf of Mexico (BOESCH et al., 2009;
123 DUAN et al., 2013). The Pearl River (PR), in contrast, is a small 3rd order black-water river that
124 is less perturbed by human activities compared with the MR. The Pearl River is 790 km long
125 with a total drainage area of about 22,690 $km^2$ covering east-central Mississippi and southeastern
126 Louisiana. The most important land type in the PR basin is natural forest (~43%), followed by
127 agricultural regions (27%) and marsh and/or swamp areas (~10%). Our sampling station was on
128 the East Pearl River (EPR) near the Stennis Space Center, the same sampling location as in many
129 previous studies (e.g., DUAN and BIANCHI, 2006; DUAN et al., 2007b; CAI and GUO, 2009;
130 SHILLER et al., 2012; WANG et al., 2013), which have provided rich background information on
131 DOM concentrations and composition and their spatial and temporal variations. SHILLER et al.
132 (2012) pointed out that, during low discharge, Hobolochitto Creek may become the primary
133 water source at the EPR depending on the specific sampling time. However, previous studies
134 have found that both DOC abundance and DOM composition did not show significant difference
135 between sampling stations on the EPR and a PR mainstem station at Bogalusa, MS although
136 spatial variation along the upper river was observed (e.g., DUAN and BIANCHI, 2006; DUAN et al.,
137 2007b).

138 St. Louis Bay (SLB) is a shallow semi-closed estuary located on the Mississippi Gulf Coast,
139 receiving freshwater inputs from the Jourdan River (JR) and the Wolf River, which are black-
140 water, forested rivers with limited human influence (Fig. 1). The abundance, distribution, and
141 mixing behaviors of nutrients and organic carbon in the SLB estuary have recently been reported
142 (WANG et al., 2010; CAI et al., 2012; LIN et al., 2012). The SLB connects to the Gulf of Mexico
143 through the Mississippi Sound (MS), where estuarine waters from SLB further mix with
144 seawater (Fig. 1). Additionally, the PR empties into the MS (CHIGBU et al., 2005) and the MR

provides a portion of the water sources into the Mississippi Bight (MB) in the northern Gulf of Mexico (Blumberg et al., 2001; MOREY et al., 2003; BRUNNER et al., 2006).

Samples from the two contrasting rivers were used to examine linkages among colloidal size/composition, DOM sources and river settings, while the estuarine samples should reveal the dynamic change in colloidal size and composition across the river-sea interface.

2.2. Sample collection

Monthly water samples were collected between January 2009 and February 2010 from the lower MR near the USGS hydrological station at Baton Rouge, Louisiana (30°26′17.01″ N, 91°11′33.14″ W) and from the EPR at Stennis Space Center, Mississippi (30°20′55.52″ N, 89°38′28.74″W, Table 1, Fig. 1). Time series samples from these two rivers should provide coupled information on DOM characteristics and hydrological conditions. Water samples were also collected along a salinity gradient from the JR (30°23′12″ N, 89°27′46″ W), through the SLB estuary, to the MS and the MB during October 2009 (Table 2, Fig. 1), to provide the first data set of DOM size distribution in the SLB estuary. For laboratory mixing experiments, end-member river water was collected from the JR, but on a different day from the field salinity gradient sampling, and end-member seawater from the MB in the northern Gulf of Mexico (Table 2, Fig. 1).

Discharge data at the hydrological stations at Baton Rouge for the lower MR and at Bogalusa for the PR were acquired from the USGS national water information system website (http://waterdata.usgs.gov/nwis/rt). There is no routinely measured discharge for the EPR. Thus, reported PR discharge here only provides a general indication of the variation pattern of the discharge due to the complex hydrology of the EPR system (SHILLER et al., 2012).

Large volumes of surface water samples (~40 L) were filtered *in situ* through a 0.45 µm Memtrex polycarbonate pleated cartridge (GE Water and Process Technologies) for ultrafiltration (see below). Aliquots of filtered waters were collected in pre-combusted glass vials for the measurements of DOC and in HDPE plastic bottles for FlFFF analysis. Samples were kept in an iced cooler and transported back to the lab within 2-3 h of collection and stored in the dark at 2˚C until further analysis. Water temperature and salinity were measured with a YSI water quality sonde at the time of sample collection.

176 2.3. Ultrafiltration

177 Ultrafiltration was used to quantify the concentration of bulk colloidal organic carbon
178 (COC). An ultrafiltration membrane having a nominal MW cutoff of 1 kilo-Dalton (kDa), which
179 corresponds to ~1.3 nm in size (GUO and SANTSCHI, 2007), was used. Time-series permeate (<1
180 kDa) samples were collected at different concentration factors (CF) and were determined for
181 DOC concentration to quantify the COC abundance (or percentage) in the bulk DOC (GUO and
182 SANTSCHI, 1996; GUO and SANTSCHI, 2007), by fitting the time-series permeate DOC
183 concentration ($C_p$) against CF:

184 $$\ln C_p = \ln\left(P_c \times C_f^0\right) + \left(1 - P_c\right) \times \ln\left(CF\right)$$

185 where $P_c$ is the permeation coefficient of low-molecular-weight (LMW) or permeable DOC,
186 defined as the ratio of $C_p$ to $C_f$ (feed concentration of permeable DOC), and $C_f^0$ is its initial feed
187 concentration. DOC recovery from permeate and retentate was, on average, 98±2% for all
188 samples.

189

190 2.4. Measurements of DOC and UV-vis absorbance

191 Concentrations of DOC were measured with a Shimadzu TOC-V total organic carbon
192 analyzer using the high temperature combustion method (GUO et al., 1995). Calibration curves
193 were generated before sample analysis. Samples were acidified with concentrated HCl to pH ≤ 2
194 before analysis. Each sample was determined with three to five replicates, each using 150 μL,
195 with a coefficient of variance < 2%. Ultrapure water, working standards and certified DOC
196 standards (from University of Miami) were measured every eight samples to check the
197 performance of the instrument and to ensure data quality (ZHOU et al., 2013). The UV-vis
198 absorption spectra of samples were measured on a Cary 300 Bio UV-vis spectrophotometer in 1-
199 cm quartz cuvettes over 200-1100 nm with 1 nm increments (ZHOU et al., 2013). Samples with
200 absorbance higher than 0.02 at 260 nm were diluted with ultrapure water (18.2 MΩ) to reach
201 absorbance <0.02 in order to minimize the inner-filter effect (COBLE et al., 1998; GUÉGUEN et al.,
202 2005). The absorbance spectrum of ultrapure water blank (measured daily) was subtracted from
203 samples' absorbance spectra.

204

205 2.5. Measurements of colloidal size spectra using FlFFF

206 The FlFFF system (Postnova F-1000) was coupled on-line with a UV-absorbance (Model
207 228, ISCO) and two fluorescence detectors (Waters Model 474 and LabAlliance Acufluor LC-
208 305). The instrumental settings for the FlFFF are shown in Table 3. Chromophoric DOM was
209 detected by measuring the UV-absorbance at 254 nm ($UV_{254}$), while humic-like and protein-like
210 DOM were detected by measuring the fluorescence at Ex/Em wavelengths of 350/450 nm
211 ($Fluo_{350/450}$) and 275/340 nm ($Fluo_{275/340}$), respectively. The analytical procedures and conditions
212 are described elsewhere (STOLPE et al., 2010; STOLPE et al., 2014) and the choice of fluorescence
213 settings was based on previous reports (COBLE et al., 1990; YAMASHITA and TANOUE, 2003;
214 COBLE, 2007). Since the size of natural DOM is mostly <10 nm (GUO and SANTSCHI, 2007), our
215 focus in this study was mainly on the colloidal size <20 nm. Therefore, the flow settings of the
216 FlFFF (Table 3) were optimized for determining the colloidal size spectrum with a high
217 resolution in the 0.5-20 nm size range. At the end of separation (~60 min), the cross flow was
218 turned off for the rapid elution and detection of the remaining colloidal materials in the >20 nm
219 range. The conversion of FlFFF retention time to diffusion coefficient and hydrodynamic
220 diameter was accomplished through calibration using proteins with known molecular weights
221 and diffusion coefficients, including ovalbumin, bovine serum albumin, ferritin and
222 thyroglobulin, under the same settings as sample analysis (STOLPE et al., 2010). Quinine sulfate
223 standards were used to quantify fluorescent DOM based on calibration curves built from a series
224 (4-5) of quinine sulfate standards using their integrated signals at $Fluo_{350/450}$ (COBLE et al., 1998;
225 STOLPE et al., 2014). Thus, absorbance and fluorescence intensities are reported in ppb-quinine
226 sulfate equivalents (ppb-QSE). Integrations of the full colloidal spectra (including the >20 nm
227 material) were used to quantify the FlFFF-recoverable colloids and are denoted as $[UV_{254}]_{FFF}$,
228 $[Fluo_{350/450}]_{FFF}$ and $[Fluo_{275/340}]_{FFF}$. The colloidal size spectra were also integrated over smaller
229 size ranges, such as the 0.5-4 nm, 4-20 nm and >20 nm, and the proportions of DOM in these
230 size intervals were calculated as fractions relative to the whole FlFFF-recoverable fraction, for
231 example, $[UV_{254}]_{0.5\text{-}4nm}/[UV_{254}]_{FFF}$.
232
233 2.6. Laboratory mixing experiment
234 Laboratory experiments were conducted to mimic the mixing between river water and
235 seawater in the SLB estuary, in order to examine the dynamic change in colloidal size spectra as
236 a result of estuarine mixing and resultant physicochemical processes. The end-member river

237 water from the JR (S=0.2) and seawater from the northern Gulf of Mexico (S=30) were mixed in
238 varying proportions to generate samples with different salinities (S = 0.2, 3, 6, 8, 10, 14, 18, 22,
239 26, and 30). The mixing samples were stored dark at 4˚C for 2 hours and then were filtered
240 through GF/F filters (0.7 μm) to remove materials that flocculated during mixing. The filtrates
241 were measured for DOC concentrations, UV absorbance, and colloidal size spectra using FlFFF.
242 Note that the DOC concentration of JR water for the mixing experiment was considerably lower
243 than that during field gradient sampling and only physicochemical processes were being tracked
244 in the short-term mixing experiment.
245
246 2.7. Data statistics
247 All statistical analyses were done in MATLAB 6.5.1 (Mathworks). One-way ANOVA tests
248 were performed to examine significance of differences of data between different sample sets.
249
250 2.8. Fluorescent DOM components from fluorescence excitation emission matrix analysis
251 The water samples used for FlFFF analysis were also measured for their fluorescent
252 properties using fluorescence excitation emission matrices (EEMs). Detailed method description
253 has been provided in ZHOU et al. (2013). In summary, EEMs were first collected covering
254 excitation and emission wavelength rages of 220-400 nm and 240-550 nm, respectively. Based
255 on the EEM data, major DOM components were then derived using parallel factor (PARAFAC)
256 analysis (ANDERSEN and BRO, 2003; STEDMON and BRO, 2008). In addition, the biological index
257 (BIX) was also determined from fluorescence EEMs as the ratio of emission between 380 and
258 430 nm under excitation at 310 nm and used as an index of autochthonous DOM (HUGUET et al.,
259 2009; BIRDWELL and ENGEL, 2010).
260
261 **3. Results**
262 3.1. Characteristics of bulk DOM in river waters
263 Concentrations of DOC in the lower MR ranged from 236 to 343 μM, with an average of
264 290 ± 37 μM (Table 1). The highest DOC concentration (343 μM) was found at the highest river
265 discharge (34,688 $m^3/s$), although no significant correlation was found between DOC and
266 discharge ($r^2$ = 0.14, $p > 0.1$). Compared to the lower MR, significantly higher DOC
267 concentrations ($p < 0.001$) were found in the EPR, ranging from 326 to 1121 μM, with an

268 average of 645 ± 230 µM (Table 1). Overall, a significant correlation was found between DOC
269 in the EPR and discharge in the Pearl River at Bogalusa ($r^2 = 0.55$, $p < 0.01$).
270 Bulk colloidal organic carbon (COC) concentrations, as quantified by the ultrafiltration
271 permeation model, ranged from 151 to 204 µM in the lower MR (average of 177 ± 20 µM, Table
272 1), comprising 57-61% of the bulk DOC. Only one sample was collected in the EPR for
273 ultrafiltration, which was during a flooding event, and the concentration of COC was 604 µM
274 (Table 1), comprising 72% of the bulk DOC.
275
276 3.2. Colloidal size spectra in river waters
277 Examples of the colloidal size spectra of the chromophoric, humic-like, and protein-like
278 DOM are shown in Fig. 2. Within the 0.5-20 nm hydrodynamic diameter ($d_H$) range,
279 chromophoric ($UV_{254}$) and humic-like DOM ($Fluo_{350/450}$) both showed one narrow peak at 0.5-4
280 nm, centered at 1.5±0.5 nm for chromophoric DOM and at 1.2 ± 0.5 nm for humic-like DOM
281 (Fig. 2). In contrast, the colloidal size spectra of protein-like DOM ($Fluo_{275/340}$) showed multiple
282 peaks. One peak at 0.5-4 nm matched the spectra of chromophoric and humic-like DOM, while
283 an additional peak occurred at 3-8 nm, centered at 4.8 ± 0.4 nm (Fig. 2). In addition, a high
284 abundance of protein-like DOM was also detected in the >20 nm range (Fig. 2). The differences
285 in colloidal size spectra of chromophoric, humic-like and protein-like DOM types indicate that
286 distinct populations of colloids with different compositions occur in the samples.
287 To better quantify the partitioning of colloids between different size ranges, the colloidal
288 size spectra were integrated over the intervals 0.5-4 nm, 4-20 nm and >20 nm, respectively. As
289 shown in Fig. 3, more than 74% of the FlFFF-recoverable chromophoric DOM and more than
290 83% of the FlFFF-recoverable humic-like DOM were found in the 0.5-4 nm size fraction in the
291 lower MR and PR. In contrast, large fractions of the FlFFF-recoverable protein-like DOM (66%
292 for the lower MR and 41% for the EPR) were found in the >20 nm size fraction (Fig. 3), again
293 showing that protein-like DOM in river waters was mostly associated with large colloids. Note
294 that the FlFFF-recoverable DOM in this study does not include the <1 kDa size fraction due to
295 the pore-size (1 kDa) of the FlFFF channel membrane. Additional terrestrial and autochthonous
296 DOM is likely to partition to the <1 kDa size fraction as well, but the reported size partitioning in
297 this study only pertains to the recoverable colloidal (>1 kDa) size fraction.
298

299 3.3. Colloidal size distribution in estuarine waters

300 Along the river-seawater transect, concentrations of DOC decreased from 1618 μM in the
301 JR to an average value of 972 μM in the SLB estuary, then to 234 μM in the MB (Table 2). As
302 shown in Fig. 4, both DOC and UV-absorbance showed a conservative mixing behavior within
303 the SLB estuary (S≤15). Beyond salinity 15 outside the SLB estuary, DOC showed a different
304 mixing trend due to the influence of different coastal waters in the MS and MB (Blumberg et al.,
305 2001). The concentrations of COC decreased from 1107 μM in the JR to 415 μM in SLB and 99
306 μM in the higher salinity waters, and also showed different mixing trends in the SLB estuary and
307 the coastal waters (Table 2). The COC% in the bulk DOC also decreased along the salinity
308 gradient from 68% in river water to 51% in estuarine and 42% in coastal waters (Table 2). The
309 absorption coefficient at 254 nm ($a_{254}$) was positively correlated with DOC ($r^2$ = 0.99,
310 $p$<0.00001) and decreased with increasing salinity (Fig. 4), showing a major DOM source from
311 river waters.

312 The abundance of colloidal chromophoric DOM quantified as $[UV_{254}]_{FFF}$ decreased from
313 1,934 ppb-QSE in the JR to an average of 380 ppb-QSE in SLB and to 26 ppb-QSE in the MB,
314 showing an evident non-conservative mixing trend (Fig. 5). Similarly, the $[UV_{254}]_{FFF}$/COC ratio
315 decreased from 1.67 g-QSE/mol-C in the JR to an average value of 0.67 g-QSE/mol-C in the
316 SLB and then to 0.23 g-QSE/mol-C in the MB (Fig. S1). As shown in Fig. 5, the abundance of
317 colloidal humic-like DOM quantified as $[Fluo_{350/450}]_{FFF}$ decreased from 8.63 ppb-QSE in the JR
318 to 2.51 ppb-QSE in SLB, and then to 0.08 ppb-QSE in the MB. In addition, the abundance of
319 protein-like DOM quantified as $[Fluo_{275/340}]_{FFF}$ generally decreased along the salinity gradient
320 (Fig. 5). The ratio of colloidal protein-like to humic-like DOM ($[Fluo_{275/340}]_{FFF}$/$[Fluo_{350/450}]_{FFF}$),
321 on the other hand, increased from 1.4 in river water to 6.1 in estuarine waters and to 13.7 in
322 coastal waters in the MB.

323

324 **4. Discussion**

325 4.1. Factors affecting the abundance of bulk DOM and COM

326 No significant correlation was found between DOC concentration and discharge in the lower
327 Mississippi River, probably due to integration of signals from multiple tributaries and mixed
328 DOM sources (BIANCHI et al., 2004; DUAN et al., 2007a; WANG et al., 2013; Cai et al., 2015). In
329 contrast, DOC concentrations were significantly correlated with river discharge in the Pearl

River, suggesting a hydrological control of the DOC-concentration relationship (DALZELL et al., 2007).

The higher COC concentration and colloidal fraction in the EPR are consistent with the higher forest coverage in the EPR drainage basin, with forest top soil contributing fresh HMW-DOM to the river (MATTSSON et al., 2005). In contrast, the lower COC concentrations and colloidal fractions in the MR were probably due to the combined effects of agricultural land contributing more degraded LMW-DOM to the river (e.g., CRONAN et al., 1999; DALZELL et al., 2011), levees restricting the inputs of terrestrial organic matter to the river, and intensive degradation (photo-chemically and/or biologically) of DOM during its long transport and residence time in dams and reservoirs (DUAN et al., 2013).

Ultrafiltration is a physical size separation with minimal sample perturbation since no carrier solution or pH adjustment is needed. However, its results provide only the abundance of bulk colloidal size fraction larger than membrane's size cutoff (GUO and SANTSCHI, 2007). In contrast, FlFFF offers continuous colloidal size separation and characterization (Zhou and Guo, 2015) although DOM conformation structure may be altered if the ionic strength and pH between the original sample and the carrier solution are different since usage of a carrier solution is necessary to minimize interactions between different analytes and between analytes and the FlFFF membrane (GIDDINGS, 1993; WILLIAMS et al., 1997; DU and SCHIMPF, 2002). Thus, caution should be taken when comparing results between ultrafiltration and FlFFF analyses (see sections below). Nonetheless, the application of both techniques should provide new insights into understanding the DOM composition and size portioning.

4.2. Factors affecting the colloidal size spectra of river and estuarine waters

It is likely that the small sized colloidal DOM at 0.5 - 4 nm was largely composed of fulvic acid, as suggested in previous studies (BECKETT et al., 1987; ZANARDI-LAMARDO et al., 2002; STOLPE et al., 2014). The smaller sized humic-like DOM compared to chromophoric DOM is consistent with other studies, and suggests the existence of light-absorbing moieties that either do not fluoresce or fluoresce less intensively at larger size fractions (ZANARDI-LAMARDO et al., 2002; STOLPE et al., 2010; GUÉGUEN and CUSS, 2011). In contrast, the protein-like DOM in the 0.5-4 nm is associated with the same type of presumed fulvic acid as the humic-like DOM in this size range. For example, it has been found that phenol-like DOM can also fluoresce at the Ex/Em

wavelengths of typical protein-like DOM (MAIE et al., 2007; HERNES et al., 2009). It is also possible that the apparent protein-like DOM (detected at Ex/Em 275/340 nm) in the 0.5-4 nm size range is an interference from the emission peak of humic-like DOM extending to the wavelength range of protein-like DOM (STOLPE et al., 2014). Additionally, previous studies showed terrestrial sources of colloidal amino acids in the lower Pearl River (DUAN et al., 2007a). The protein-like colloids in the 3-8 nm and >20 nm size ranges are likely derived from *in situ* production since it has been shown that protein-like DOM in rivers is mainly derived from autochthonous sources, (FELLMAN et al., 2010; WILLIAMS et al., 2010) and freshly produced DOM is typically larger in size than more degraded and humic-like DOM (AMON and BENNER, 1996).

Our results on the size partitioning of humic-like DOM are similar to those observed in other aquatic systems (GUÉGUEN and CUSS, 2011). In addition, our finding that the >20 nm fraction comprised a larger portion of the protein-like DOM in the lower MR than in the EPR agrees with the higher autochthonous DOM production in the MR (DUAN et al., 2007a; Cai et al., 2015) and the larger size of fresh autochthonous DOM as compared with more degraded DOM (AMON and BENNER, 1996).

By integrating the whole colloidal size spectrum of chromophoric DOM, the abundance of FlFFF-recoverable colloidal chromophoric DOM ($[UV_{254}]_{FFF}$) can be calculated. Lower MR waters had $[UV_{254}]_{FFF}$ values ranging from 36 ppb-QSE during low flow to 261 ppb-QSE during high flow (average of 137 ppb-QSE, Fig. S2). No significant correlation was found between $[UV_{254}]_{FFF}$ and discharge ($r^2 < 0.01$, $p > 0.05$, Fig. S2) or between $[UV_{254}]_{FFF}$ and DOC concentration ($r^2 < 0.05$, $p > 0.1$, Fig. S3) in the lower MR, indicating the lack of a simple hydrological control on colloidal chromophoric DOM and/or higher existence of non-chromophoric colloidal DOM in the river. Values of $[UV_{254}]_{FFF}$ in the EPR ranged from 123 ppb-QSE during base flow to 4267 ppb-QSE during flood season, with an average of 1197 ppb-QSE (Figs. S3 and S4), which is considerably higher ($p < 0.005$) than in the lower MR. The correlation between $[UV_{254}]_{FFF}$ in the EPR and discharge in the Pearl River at Bogalusa ($r^2=0.71$, $p < 0.002$, Fig. S2) was stronger than the correlation between bulk DOC and discharge ($r^2 = 0.55$, $p < 0.01$). Thus, the input of colloidal chromophoric DOM to the river, and its contribution to the total DOC pool increased during high discharge probably as a result of increased soil leaching and surface water runoff. A stronger correlation between $[UV_{254}]_{FFF}$ and DOC was found in the

EPR ($r^2$=0.43) than in the lower MR ($r^2$=0.05, Fig. S3), indicating that the chromophoric colloidal component was more important in the EPR than in the lower MR. This observation can be explained by the higher forest coverage in the EPR drainage basin, with forest top soil contributing highly aromatic DOM to the river (DUAN et al., 2007a).

The ratio between $[UV_{254}]_{FFF}$ and COC has been used as the counterpart to $SUVA_{254}$ (the ratio of UV absorbance to DOC concentration), representing aromaticity of colloidal organic matter (WEISHAAR et al., 2003; STOLPE et al., 2010), although their absolute values are not comparable. The $[UV_{254}]_{FFF}$/COC ratio in the lower MR ranged from 0.18 to 1.00 g-QSE/mol-C with an average of 0.57 g-QSE/mol-C, and was 4.50 g-QSE/mol-C in the sample collected during a flood event (April 07, 2009) in the EPR. Considerably higher $[UV_{254}]_{FFF}$/COC ratio in the EPR indicates greater aromaticity of colloidal DOM in the EPR than the MR, which is consistent with the higher importance of lignin-phenols, an aromatic biomarker for terrestrial organic matter, in the EPR compared to the MR (DUAN et al., 2007a).

The proportion of colloidal humic-like DOM in the bulk DOM was quantified by the ratio of $[Fluo_{350/450}]_{FFF}$ to the bulk DOC. In the lower MR, the $[Fluo_{350/450}]_{FFF}$/DOC ratio ranged from 0.00012-0.010 g-QSE/mol-C with an average of 0.0049 g-QSE/mol-C (Fig. S3). Similar to the bulk DOC and other colloidal components, no significant correlation with discharge was found for $[Fluo_{350/450}]_{FFF}$, possibly due to diverse sources and multiple controlling factors of humic-like colloidal DOM in the MR basin. In the EPR, the $[Fluo_{350/450}]_{FFF}$/DOC ratio ranged from 0.0022-0.039 g-QSE/mol-C (averaging 0.014 g-QSE/mol-C), which was significantly greater than in the lower MR ($p$ <0.01). In addition, $[Fluo_{350/450}]_{FFF}$/DOC was significantly correlated with discharge in the PR ($r^2$ = 0.43, $p$ < 0.01), suggesting increased importance of humic substances in the bulk DOM pool with increasing discharge in the PR.

The relative importance of colloidal protein-like DOM in comparison with colloidal chromophoric DOM can be evaluated by the ratio of $[Fluo_{275/340}]_{FFF}$ to $[UV_{254}]_{FFF}$ (Fig. S3). Samples from the lower MR had $[Fluo_{275/340}]_{FFF}$ /$[UV_{254}]_{FFF}$ ratios ranging from 0.011-0.090 (mean = 0.035), while samples from the EPR had $[Fluo_{275/340}]_{FFF}$ /$[UV_{254}]_{FFF}$ ratios ranging from 0.0024 to 0.048 (mean = 0.013). Significantly lower $[Fluo_{275/340}]_{FFF}$ /$[UV_{254}]_{FFF}$ ratios in the EPR ($p$ <0.005) point to a compositional difference between lower MR and EPR waters, with more in situ phytoplankton production and thus more protein-like colloidal DOM in lower MR waters, and more soil-derived humic-like DOM from the EPR. This is consistent with previous

observations using other techniques and/or biomarkers for the lower MR and EPR (DUAN et al., 2007a; DUAN et al., 2013). Interestingly, the $[Fluo_{275/340}]_{FFF}/[UV_{254}]_{FFF}$ ratio exhibited a negative correlation with discharge in the MR ($r^2$=0.59, p<0.005,), but showed no correlation with discharge in the EPR. The decrease in $[Fluo_{275/340}]_{FFF}/[UV_{254}]_{FFF}$ ratio with increasing discharge in the lower MR suggests different sources of colloidal chromophoric and protein-like DOM. As previously hypothesized, a major source of colloidal chromophoric DOM was from the leaching of soil and plant litter during high flow, while colloidal protein-like DOM was mostly autochthonous in nature and subject to dilution during high flow.

Correlations were found between DOM components at specific size ranges derived from FlFFF and fluorescent DOM components derived from fluorescence EEMs and PARAFAC analysis. As shown in Fig. S4, representative fluorescent DOM components identified from EEMs in the two rivers (detected and modeled from the same water samples for FlFFF analysis) include a humic-like (Component-1, C1, upper panel) and a protein-like (Component-6, C6, lower panel) component. The proportion of humic-like DOM found in the 0.5-4 nm size fraction can be expressed as the $[Fluo_{350/450}]_{0.5\text{-}5nm\text{-}FFF}$/DOC ratio, and was positively correlated to the percentage of fluorescent DOM associated with C1 (C1%) in both MR ($r^2$ = 0.49, $p$ < 0.01) and EPR waters ($r^2$ = 0.33, $p$ = 0.05). This suggests that the 0.5-4 nm humic-like colloids represent a considerable portion of C1 and/or exhibited similar behavior as C1. In the MR, the relative importance of protein-like DOM in the >20 nm fraction ($[Fluo_{275/340}]_{>20nm\text{-}FFF}$/DOC) was positively correlated ($r^2$= 0.45, $P$ = 0.01) with the percentage of fluorescent DOM associated with C6 (C6%) (Fig. S5). Again, this further suggests the protein-like C6 mostly partitioned to larger (>20 nm) size ranges and/or behaved similarly as larger-sized protein-like DOM in the MR. In the EPR, no correlation was found between $[Fluo_{275/340}]_{>20nm\text{-}FFF}$/DOC and C6% ($r^2$= 0.02, $p$ = 0.63), likely due to lesser degree of DOM reworking and lower existence of protein-like DOM compared with the lower MR. The correlation between results found in FlFFF and fluorescence EEM analyses shows compatibility and confirmation of the findings from the two methods, and provides new insights into the composition and size distribution of DOM in natural waters.

The colloidal size spectra of chromophoric and humic-like DOM in the JR and the SLB estuary showed a major narrow peak at 0.5-4 nm, similar to the observations in the MR and EPR samples (Fig. 2). It is likely that the chromophoric and humic-like colloidal DOM in the SLB

estuary was associated with the same type of presumed fulvic acid colloids as in the rivers. Integration of the colloidal size spectra over different size ranges showed that proportion of the FlFFF recoverable humic-like DOM in the 0.5-4 nm size fraction decreased from 89% in the JR to an average value of 83% in SLB and to 72% in the MB (Fig. 6), suggesting a slight shift in the size of colloidal humic substances from small to large sizes as the salinity increased. The colloidal size spectra of protein-like DOM showed two peaks in the 0.5-4 nm and 3-8 nm size ranges, but the major portion of the colloidal protein-like DOM was associated with the >20 nm materials (Fig. 2). The percentage of the FlFFF-recoverable protein-like DOM found in the >20 nm size fraction increased from 60% in the JR, to 61% in SLB, and ~71% in the MB (Fig. 6), showing increased importance of large-sized protein-like colloids in coastal waters. This observation agrees well with our hypothesis that the medium and large sized protein-like colloids are formed by *in situ* production. In addition, the >20 nm colloids could be formed through the flocculation of smaller colloids during estuarine mixing (SHOLKOVITZ, 1976) (see also discussion below).

The decrease in the abundance of colloidal chromophoric DOM and the $[UV_{254}]_{FFF}$/COC ratio with salinity indicate a decrease in the abundance and loss in aromaticity of colloidal DOM from river to estuary and to coastal waters. Figure 5 shows that the abundance of protein-like colloidal DOM decreased by a slower rate than humic-like colloidal DOM going from river water to coastal seawater, and is likely the result of an additional source of protein-like DOM from marine production. There is a seeming deviation from the general increasing trend at mid-salinity (S ~15), where $[Fluo_{275/340}]_{FFF}/[Fluo_{350/450}]_{FFF}$ is higher than what would be expected based on the trend observed at all the other stations. Fluorescence EEM results show that a similar positive deviation of the biological index (BIX), an index representing autochthonous sources, was also observed at this station (Fig. S6), indicating a higher proportion of autochthonous DOM at this mid-salinity station. Additionally, the highest chlorophyll-a concentration was found in the same region in the MS at this season (STOLPE et al., 2014). Thus, the high ratio between protein-like and humic-like DOM observed at mid- and higher-salinity stations in the study area was probably a result of high *in situ* DOM production.

### 4.3. Mixing behavior of different sized colloidal DOM in estuarine waters

The mixing behavior of DOC has been widely reported in Gulf of Mexico estuaries, showing conservative, addition, or removal behavior (GUO and SANTSCHI, 1997b; GUO et al., 1999; WANG et al., 2010). Nevertheless, to the best of our knowledge, there are no studies reporting the estuarine mixing behavior of colloids in different sizes incorporating both field studies and laboratory mixing experiments. As shown in Fig. 4 for the bulk DOC and $a_{254}$ in the field samples, there was an apparent DOC removal over the entire salinity range, from the JR to SLB and extending to MS and MB. However, a closer look at these data reveals that within the SLB estuary (salinity ≤15), the bulk DOC actually had a conservative mixing behavior (Fig. 4). As pointed out by WANG et al. (2010), the apparent removal of bulk DOC in the waters outside SLB is largely due to the occurrence of different coastal waters with different DOC endmember concentrations, resulting in a two-segment mixing trend.

In contrast to the conservative mixing observed for the bulk DOC, the colloidal chromophoric DOM ($[UV_{254}]_{FFF}$) indeed showed significant removal within the SLB estuary (Fig. 5). Chromophoric DOM in the 0.5-4 nm size fraction ($[UV_{254}]_{0.5\text{-}4nm}$) also showed the same trend as $[UV_{254}]_{FFF}$ or the bulk colloidal chromophoric DOM in the field samples (Fig. 7), since most of the FlFFF-recoverable chromophoric DOM partitioned to the 0.5-4 nm size range (section 3.3). However, similar to the bulk DOC, the colloidal humic-like DOM ($[Fluo_{350/450}]_{FFF}$) and humic-like DOM in the 0.5-4 nm size range ($[Fluo_{350/450}]_{0.5\text{-}4nm}$) seemed to exhibit conservative behavior within SLB with a salinity <15 (Figs. 5 and 7), showing distinct estuarine mixing behavior among colloids with different composition and sizes.

Similar to the field data, laboratory mixing experiments using end-member river water (DOC: 387 μM; $[UV_{254}]_{FFF}$: 321 ppb-QSE) and seawater (S = 30; DOC: 154 μM; $[UV_{254}]_{FFF}$: 37 ppb-QSE) also showed conservative mixing behaviors of DOC and $a_{254}$ values (Fig. 4), but a removal of $[UV_{254}]_{FFF}$ and $[UV_{254}]_{0.5\text{-}4nm}$ with increasing salinity (Figs. 5 and 7). Also similar to the field data, the humic-like DOM in both the bulk colloidal ($[Fluo_{350/450}]_{FFF}$) and the 0.5-4 nm size fraction ($[Fluo_{350/450}]_{0.5\text{-}4nm}$) demonstrated an overall conservative mixing behavior (Figs. 5 and 7). Similar results observed between field data and laboratory mixing experiments suggest that physicochemical processes, such as sea salt-induced flocculation/coagulation, play the major role in regulating the mixing behavior of DOC and colloidal DOM in the estuary since the short-term laboratory mixing experiment (2 h) likely excluded biological effects. Note that the JR sampling for the mixing experiment was carried out at a different time from that of the field

study due to the labor-intensive nature for both FlFFF analysis and ultrafiltration and the necessity to keep the samples fresh and measured as soon as possible. Unfortunately, DOC concentrations between the two sampling trips differed considerably. It is thus possible that the specific behavior of colloidal DOM in the mixing experiment was not exactly the same as that observed during field study. However, although DOC concentrations in the Jourdan River, a small forested river, were considerably different between the field study (1618 µmol/L) and the laboratory mixing experiment (387µmol/L), the DOM composition can be expected to be similar and the behavior of the DOM during estuarine mixing should be comparable.

As shown in Fig. 8, the colloidal protein-like DOM ($Fluo_{275/340}$) in samples from laboratory mixing experiments was mostly partitioned to the >20 nm size fraction with a bi-modal size distribution in the low nm size range. The relative importance of the mid-size colloids (4-8 nm) as compared to the small size colloids (0.5-4 nm) increased with salinity (Fig. 8). In the end-member coastal seawater (S = 30) and high salinity mixed sample (e.g., S = 26), the size spectra of protein-like DOM in the low nanometer size range did not show a distinct bi-modal distribution (Fig. 8). Instead, they were characterized by one very wide peak from 0.5 to 15 nm (centered at 5-7 nm), reflecting a change in relative importance of protein-like DOM in different colloidal sizes from river to coastal waters (Fig. 9).

Integration of the colloidal size ranges showed that the abundance of protein-like DOM in small, mid- and large size fractions all decreased as salinity increased in the mixing experiment (Fig. 9). The small-sized protein-like DOM ($[Fluo_{275/340}]_{0.5\text{-}4nm}$) showed an apparent removal pattern (Fig. 9), similar to that of chromophoric DOM in this size range. As opposed to the small size colloids, the mid-sized protein-like DOM ($[Fluo_{275/340}]_{4\text{-}8nm}$) seemed to behave conservatively, especially in the low salinity range (Fig. 9). The wide peak of protein-like DOM in the low nanometer size range at high salinity as described above (Fig. 8) led to difficulties in a clear-cut separation of the small and mid-sized protein-like DOM and may have resulted in the scattered relationship of $[Fluo_{275/340}]_{4\text{-}8nm}$ with salinity in the higher salinity range. The >20 nm protein-like DOM ($[Fluo_{275/340}]_{>20nm}$) showed removal behavior at low salinity during mixing (Fig. 9). It thus appears that the mid-sized protein-like DOM did not undergo significant flocculation while the small and large size fractions were affected by salt-induced flocculation. Both the ratio of $[Fluo_{275/340}]_{4\text{-}8nm}/[Fluo_{275/340}]_{0.5\text{-}4nm}$ and ratio of $[Fluo_{275/340}]_{>20nm}/[Fluo_{275/340}]_{0.5\text{-}4nm}$ increased with increasing salinity (Fig. 10, right panels), possibly linked to the transformation

546 from small colloids to mid-sized colloids and large size colloids during estuarine mixing.
547 However, this trend was less obvious in the field samples (Fig. 10, left panels). Highest
548 $[Fluo_{275/340}]_{4\text{-}8nm}/[Fluo_{275/340}]_{0.5\text{-}4nm}$ ratio was found at salinity 15, corresponding to relatively high
549 $[Fluo_{275/340}]_{FFF}/[Fluo_{350/450}]_{FFF}$ ratio and BIX (Fig. 5 and Fig. S6), suggesting a source from
550 freshly produced marine DOM. Previous work using size exclusion chromatography also
551 separated protein-like DOM in the nanometer size range into two fractions and related the
552 smaller one (~7 kDa, ~2.5 nm) with phenolic moieties of humic substances and the larger one
553 (~50 kDa, ~4.5 nm) with proteinaceous DOM (MAIE et al., 2007) . Similarly, MAIE et al. (2007)
554 observed the ratio of 50 kDa to 7 kDa DOM fractions to be higher in coastal water of Florida
555 Bay than in riverine/estuarine waters. DOM in different size fractions was clearly associated
556 with distinct types of moieties. As shown in Fig. 10, the ratio of $[Fluo_{275/340}]_{>20nm}/[Fluo_{275/340}]_{0.5\text{-}4nm}$
557 also had its highest value at salinity ~15, suggesting autochthonous sources of the large size
558 (>20 nm) protein-like DOM in this region.
559 Overall, the colloidal DOM size distributions measured in the laboratory mixing
560 experiments resembled those observed in the natural estuarine samples. For example,
561 chromophoric DOM showed removal in both the field study and laboratory mixing experiments,
562 while humic-like DOM was more conservative inside the SLB and during laboratory mixing (Fig.
563 7). Physical mixing and salt-induced flocculation thus played an important role in governing the
564 fate and transport of colloidal DOM in the estuary. Protein-like DOM, on the other hand, was
565 characterized as autochthonous source in the 4-8 nm and >20 nm size intervals.
566
567 **5. Conclusions**
568 Dissolved organic matter in the lower MR was characterized by its low abundance, low
569 aromaticity and weak correlations with discharge, resulting from diverse DOM sources from
570 tributaries in the river basin, degradation and modification of DOM during transport, and
571 autochthonous sources from *in situ* production. Seasonal variations of colloidal DOM in the
572 lower MR featured a decrease in the ratio of protein-like DOM to chromophoric DOM with
573 increasing discharge, suggesting autochthonous sources of protein-like DOM that were subject to
574 dilution during high flow. More optically active DOM was found in the large sized fractions
575 (>20 nm) in the lower MR, compared to the EPR, where higher abundances of bulk DOM and
576 humic-like DOM were observed, the latter of which occurred mostly in the <4 nm size fraction.

These observations are consistent with the longer residence time and higher *in situ* production in the lower MR, and the difference in the sources of colloidal DOM is coherent with the drainage basin size, land use, and human influences on the two rivers.

In the SLB estuary, the abundance, aromaticity and relative importance of humic-like colloidal DOM decreased with salinity. However, the ratio of protein-like to humic-like colloidal DOM increased with increasing salinity, suggesting addition of autochthonous DOM and/or removal of humic-like DOM during estuarine mixing. Consistent with field observations, results from a laboratory mixing experiment clearly showed removal of the small sized colloidal chromophoric and fluorescent DOM, indicating salt-induced flocculation/coagulation during estuarine mixing in the SLB estuary. Most importantly, colloids with different sizes and composition exhibited different behaviors during estuarine mixing, with dynamic transformation between different size fractions in the estuary.

Two major types of colloids seemed to be present in coastal seawater. One type had a narrow peak at 0.5-4 nm in size showing chromophoric and fluorescent properties and was likely composed of natural fulvic acids. The other type of colloids were protein-like DOM with a larger size in the 4-8 nm and >20 nm ranges, mostly derived from *in situ* biological production. Different colloidal components exhibited distinct size spectra or size distributions. Therefore, colloidal size distributions of specific types of DOM characterized by the flow field-flow fractionation technique should provide new insights into better understanding of the transport and cycling pathways of natural organic matter in river, estuarine and coastal waters.

**Acknowledgments**

We would like to thank Kevin Martin, Xuri Wang, and Peng Lin for their assistance during sample collection. We also thank Associate Editor, Thomas Bianchi, and three anonymous reviewers for their constructive comments which improved the manuscript. This work was supported in part by funding from NOAA through the Northern Gulf Institute (Projects #09-NGI-04 and 09-NGI-13), the National Science Foundation (OCE#0850957 and OCE-MRI#1233192), and the University of Wisconsin-Milwaukee.

606 References:


607 Aiken, G. R., Hsu-Kim, H., and Ryan, J. N., 2011. Influence of Dissolved Organic Matter on the
608 Environmental Fate of Metals, Nanoparticles, and Colloids. *Environ. Sci. Technol.* **45**,
609 3196-3201, doi:10.1021/es103992s.
610 Amon, R. M. W. and Benner, R., 1996. Bacterial utilization of different size classes of dissolved
611 organic matter. *Limnol. Oceanogr.* **41**, 41-51.
612 Andersen, C. M. and Bro, R., 2003. Practical aspects of PARAFAC modeling of fluorescence
613 excitation-emission data. *J. Chemometr.* **17**, 200-215, doi:10.1002/cem.790.
614 Baalousha, M., Stolpe, B., and Lead, J. R., 2011. Flow field-flow fractionation for the analysis
615 and characterization of natural colloids and manufactured nanoparticles in environmental
616 systems: A critical review. *J. Chromatogr. A.* **1218**, 4078-4103.
617 Bauer, J. E., Cai, W.-J., Raymond, P. A., Bianchi, T. S., Hopkinson, C. S., and Regnier, P. A. G.,
618 2013. The changing carbon cycle of the coastal ocean. *Nature* **504**, 61-70.
619 Beckett, D. C. and Pennington, C. H., 1986. Water quality, macroinvertebrates, larval fishes, and
620 fishes of the lower mississippi river - a synthesis. Waterways Experiment Station,
621 Vicksburg, MS.
622 Beckett, R., Jue, Z., and Giddings, J. C., 1987. Determination of molecular weight distributions
623 of fulvic and humic acids using flow field-flow fractionation. *Environ. Sci. Technol.* **21**,
624 289-295.
625 Benedetti, M. F., Mounier, S., Filizola, N., Benaim, J., and Seyler, P., 2003. Carbon and metal
626 concentrations, size distributions and fluxes in major rivers of the Amazon basin.
627 *Hydrological Processes* **17**, 1363-1377.
628 Benner, R. and Amon, R. M. W., 2015. The Size-Reactivity Continuum of Major Bioelements in
629 the Ocean. *Ann. Rev. Mar. Sci.* **7**, DOI: 10.1146/annurev-marine-010213-135126.
630 Bianchi, T., 2007. *Biogeochemistry of estuaries*. Oxford University Press, New York.
631 Bianchi, T. S., Filley, T., Dria, K., and Hatcher, P. G., 2004. Temporal variability in sources of
632 dissolved organic carbon in the lower Mississippi river. *Geochim. Cosmochim. Ac.* **68**,
633 959-967.
634 Birdwell, J. E. and Engel, A. S., 2010. Characterization of dissolved organic matter in cave and
635 spring waters using UV,ÄìVis absorbance and fluorescence spectroscopy. *Org. Geochem.*
636 **41**, 270-280.
637 Boesch, D. F., Boynton, W. R., Crowder, L. B., Diaz, R. J., Howarth, R. W., Mee, L. D., Nixon,
638 S. W., Rabalais, N. N., Rosenberg, R., Sanders, J. G., Scavia, D., and Turner, R. E., 2009.
639 Nutrient Enrichment Drives Gulf of Mexico Hypoxia. *Eos Trans. AGU* **90**, 117-118.
640 Brunner, C. A., Beall, J. M., Bentley, S. J., and Furukawa, Y., 2006. Hypoxia hotspots in the
641 Mississippi Bight. *The Journal of Foraminiferal Research* **36**, 95-107.
642 Cai, Y. and Guo, L., 2009. Abundance and variation of colloidal organic phosphorus in riverine,
643 estuarine, and coastal waters in the northern Gulf of Mexico. *Limnol. Oceanogr.* **54**,
644 1393-1402, doi: 10.4319/lo.2009.54.4.1393.
645 Cai, Y., Guo, L., Wang, X., Mojzis, A. K., and Redalje, D. G., 2012. The source and distribution
646 of dissolved and particulate organic matter in the Bay of St. Louis, northern Gulf of
647 Mexico. *Estuarine, Coast. Shelf Sci.* **96**, 96-104. doi: 10.1016/j.ecss.2011.10.017
648 Cai, Y., Guo, L., Wang, X., and Aiken, G. 2015, Abundance, stable isotopic composition, and
649 export fluxes of DOC, POC, and DIC from the Lower Mississippi River during 2006–
650 2008, *J. Geophys. Res. Biogeosci.*, **120**, 2273-2288. doi:10.1002/2015JG003139.

Chigbu, P., Gordon, S., and Strange, T. R., 2005. Fecal coliform bacteria disappearance rates in a north-central Gulf of Mexico estuary. *Estuarine, Coastal and Shelf Science* **65**, 309-318.

Coble, P. G., 2007. Marine Optical Biogeochemistry: The Chemistry of Ocean Color. *Chemical Reviews* **107**, 402-418.

Coble, P. G., Del Castillo, C. E., and Avril, B., 1998. Distribution and optical properties of CDOM in the Arabian Sea during the 1995 Southwest Monsoon. *Deep-sea. Res. Pt. II.* **45**, 2195-2223, doi:10.1016/s0967-0645(98)00068-x.

Coble, P. G., Green, S. A., Blough, N. V., and Gagosian, R. B., 1990. Characterization of dissolved organic matter in the Black Sea by fluorescence spectroscopy. *Nature* **348**, 432-435.

Cronan, C. S., Piampiano, J. T., and Patterson, H. H., 1999. Influence of Land Use and Hydrology on Exports of Carbon and Nitrogen in a Maine River Basin. *J. Environ. Qual.* **28**, 953-961.

Dalzell, B. J., Filley, T. R., and Harbor, J. M., 2007. The role of hydrology in annual organic carbon loads and terrestrial organic matter export from a midwestern agricultural watershed. *Geochim. Cosmochim. Ac.* **71**, 1448-1462.

Dalzell, B. J., King, J. Y., Mulla, D. J., Finlay, J. C., and Sands, G. R., 2011. Influence of subsurface drainage on quantity and quality of dissolved organic matter export from agricultural landscapes. *J. Geophys. Res.* **116**, G02023.

Du, Q. and Schimpf, M. E., 2002. Correction for Particle-Wall Interactions in the Separation of Colloids by Flow Field-Flow Fractionation. *Anal. Chem.* **74**, 2478-2485.

Duan, S., Allison, M. A., Bianchi, T. S., McKee, B. A., Shiller, A. M., Guo, L., and Rosenheim, B., 2013. Transport and biogeochemical cycles of organic carbon and nutrients in the lower Mississippi River In: Bianchi, T. S., Allison, M. A., and Cai, W.-j. Eds.), *Biogeochemical Dynamics at Major River-Coastal Interfaces: Linkages with Global Change*. Cambridge University Press, New York, USA.

Duan, S. and Bianchi, T., 2006. Seasonal changes in the abundance and composition of plant pigments in particulate organic carbon in the lower Mississippi and Pearl Rivers. *Estuaries and Coasts* **29**, 427-442.

Duan, S., Bianchi, T. S., and Sampere, T. P., 2007a. Temporal variability in the composition and abundance of terrestrially-derived dissolved organic matter in the lower Mississippi and Pearl Rivers. *Mar. Chem.* **103**, 172-184, doi: 10.1016/j.marchem.2006.07.003.

Duan, S., Bianchi, T. S., Shiller, A. M., Dria, K., Hatcher, P. G., and Carman, K. R., 2007b. Variability in the bulk composition and abundance of dissolved organic matter in the lower Mississippi and Pearl rivers. *Journal of Geophysical Research* **112**, G02024, doi: 10.1029/2006JG000206.

Fellman, J. B., Hood, E., and Spencer, R. G. M., 2010. Fluorescence spectroscopy opens new windows into dissolved organic matter dynamics in freshwater ecosystems: A review. *Limnol. Oceanogr.* **55**, 2452–2462.

Giddings, J. C., 1993. Field-flow fractionation: analysis of macromolecular, colloidal, and particulate materials. *Science* **260**, 1456-1465.

Goolsby, D. A. and Battaglin, W. A., 2001. Long-term changes in concentrations and flux of nitrogen in the Mississippi River Basin, USA. *Hydrological Processes* **15**, 1209-1226, doi: 10.1002/hyp.210.

695 Goolsby, D. A., Battaglin, W. A., Aulenbach, B. T., and Hooper, R. P., 2000. Nitrogen flux and
696 sources in the Mississippi River Basin. *Sci. Total. Environ.* **248**, 75-86, doi:
697 10.1016/s0048-9697(99)00532-x.
698 Guéguen, C. and Cuss, C. W., 2011. Characterization of aquatic dissolved organic matter by
699 asymmetrical flow field-flow fractionation coupled to UV-Visible diode array and
700 excitation emission matrix fluorescence. *J. Chromatogr. A.* **1218**, 4188-4198,
701 10.1016/j.chroma.2010.12.038.
702 Guéguen, C., Guo, L., and Tanaka, N., 2005. Distributions and characteristics of colored
703 dissolved organic matter in the Western Arctic Ocean. *Continental Shelf Research* **25**,
704 1195-1207. doi: 10.1016/j.csr.2005.01.005.
705 Guo, L. and Santschi, P. H., 1996. A critical evaluation of the cross-flow ultrafiltration technique
706 for sampling colloidal organic carbon in seawater. *Mar. Chem.* **55**, 113-127.
707 doi:10.1016/S0304-4203(96)00051-5.
708 Guo, L. and Santschi, P. H., 1997a. Composition and cycling of colloids in marine environments.
709 *Rev. Geophys.* **35**, 17-40.
710 Guo, L. and Santschi, P. H., 1997b. Isotopic and elemental characterization of colloidal organic
711 matter from the Chesapeake Bay and Galveston Bay. *Mar. Chem.* **59**, 1-15.
712 Guo, L. and Santschi, P. H., 2007. Ultrafiltration and its applications to sampling and
713 characterisation of aquatic colloids. In: IUPAC Series on Analytical and Physical
714 Chemistry of Environmental Systems (Wilkinson, K.J. and Lead, J.R. Eds.),
715 Environmental colloids and particles. Chapter 4, p159-221, John Wiley and Sons, Ltd.
716 Guo, L., Santschi, P. H., and Bianchi, T. S., 1999. Dissolved organic matter in estuaries of the
717 Gulf of Mexico. *Biogeochemistry of Gulf of Mexico estuaries. Wiley*, 222-240.
718 Guo, L., Santschi, P. H., Cifuentes, L. A., Trumbore, S. E., and Southon, J., 1996. Cycling of
719 high-molecular-weight dissolved organic matter in the Middle Atlantic Bight as revealed
720 by carbon isotopic ($^{13}C$ and $^{14}C$) signatures. *Limnol. Oceanogr.* **41**, 1242-1252. doi:
721 10.4319/lo.1996.41.6.1242.
722 Guo, L., Santschi, P. H., and Warnken, K. W., 1995. Dynamics of dissolved organic carbon
723 (DOC) in oceanic environments. *Limnol. Oceanogr.* **40**, 1392-1403. doi:
724 10.4319/lo.1995.40.8.1392.
725 Hansell, D. A., 2013. Recalcitrant dissolved organic carbon fractions. *Ann. Rev. Mar. Sci.* **5**, 421-
726 445. doi: 10.1146/annurev-marine-120710-100757.
727 Hedges, J. I., 2002. Why dissolved organic matter? In: Hansell, D. A. and Carlson, C. A. Eds.),
728 *Biogeochemistry of marine dissolved organic matter*. Academic Press: San Diego,
729 London, UK.
730 Hernes, P. J., Bergamaschi, B. A., Eckard, R. S., and Spencer, R. G. M., 2009. Fluorescence-
731 based proxies for lignin in freshwater dissolved organic matter. *J. Geophys. Res.:*
732 *Biogeosci.* **114**, G00F03.
733 Honeyman, B. D. and Santschi, P. H., 1989. A Brownian-pumping model for oceanic trace metal
734 scavenging: Evidence from Th isotopes. *Journal of Marine Research* **47**, 951-992.
735 Huguet, A., Vacher, L., Relexans, S., Saubusse, S., Froidefond, J. M., and Parlanti, E., 2009.
736 Properties of fluorescent dissolved organic matter in the Gironde Estuary. *Org. Geochem.*
737 **40**, 706-719, doi: 10.1016/j.orggeochem.2009.03.002.
738 Keown, M. P., Dardeau, E. A., Jr., and Causey, E. M., 1986. Historic Trends in the Sediment
739 Flow Regime of the Mississippi River. *Water Resour. Res.* **22**, 1555-1564, doi:
740 10.1029/WR022i011p01555.

741 Lead, J. R. and Wilkinson, K. J., 2006. Aquatic Colloids and Nanoparticles: Current Knowledge
742 and Future Trends. *Environ. Chem.* **3**, 159-171.
743 Lin, P., Chen, M., and Guo, L., 2012. Speciation and transformation of phosphorus and its
744 mixing behavior in the Bay of St. Louis estuary in the northern Gulf of Mexico. *Geochim.*
745 *Cosmochim. Ac.* **87**, 283-298. doi: 10.1016/j.gca.2012.03.040.
746 Lyvén, B**,** Hassellöv, M., Haraldsson, C. and Turner, D. R. 1997. Optimisation of on-channel
747 preconcentration in flow field-flow fractionation for the determination of size
748 distributions of low molecular weight colloidal material in natural waters. *Anal. Chim.*
749 *Acta* **357**, 187-196.
750 Maie, N., Scully, N. M., Pisani, O., and Jaffé, R., 2007. Composition of a protein-like
751 fluorophore of dissolved organic matter in coastal wetland and estuarine ecosystems.
752 *Water. Res.* **41**, 563-570, doi:10.1016/j.watres.2006.11.006.
753 Mantoura, R. F. C. and Woodward, E. M. S., 1983. Conservative behaviour of riverine dissolved
754 organic carbon in the Severn Estuary: chemical and geochemical implications. *Geochim.*
755 *Cosmochim. Ac.* **47**, 1293-1309.
756 Mattsson, T., Kortelainen, P., and Raike, A., 2005. Export of DOM from Boreal Catchments:
757 Impacts of Land Use Cover and Climate. *Biogeochemistry* **76**, 373-394.
758 Meade, R. H., Yuzyk, T. R., and Day, T. J., 1990. Movement and storage of sediment in rivers of
759 the United States and Canada. In: Wolman, M. G. and Riggs, H. C. Eds.), *Surface Water*
760 *Hydrology*. Geological Society of America, Boulder, Colorado.
761 Morey, S. L., Schroeder, W. W., O'Brien, J. J., and Zavala-Hidalgo, J., 2003. The annual cycle of
762 riverine influence in the eastern Gulf of Mexico basin. *Geophys. Res. Lett.* **30**, 1867.
763 Philippe, A. and Schaumann, G. E., 2014. Interactions of Dissolved Organic Matter with Natural
764 and Engineered Inorganic Colloids: A Review. *Environ. Sci. Technol.* **48**, 8946-8962.
765 Shiller, A. M., Shim, M.-J., Guo, L., Bianchi, T. S., Smith, R. W., and Duan, S., 2012. Hurricane
766 Katrina impact on water quality in the East Pearl River, Mississippi. *Journal of*
767 *Hydrology* **414-415**, 388-392.
768 Sholkovitz, E. R., 1976. Flocculation of dissolved organic and inorganic matter during the
769 mixing of river water and seawater. *Geochim. Cosmochim. Ac.* **40**, 831-845.
770 Stedmon, C. A. and Bro, R., 2008. Characterizing dissolved organic matter fluorescence with
771 parallel factor analysis: a tutorial. *Limnol. Oceanogr.: Methods* **6**, 572-579,
772 doi:10.4319/lom.2008.6.572.
773 Stolpe, B., Guo, L., Shiller, A. M., and Aiken, G. R., 2013. Abundance, size distributions and
774 trace-element binding of organic and iron-rich nanocolloids in Alaskan rivers, as revealed
775 by field-flow fractionation and ICP-MS. *Geochim. Cosmochim. Ac.* **105**, 221-239.
776 Stolpe, B., Guo, L., Shiller, A. M., and Hassellöv, M., 2010. Size and composition of colloidal
777 organic matter and trace elements in the Mississippi River, Pearl River and the northern
778 Gulf of Mexico, as characterized by flow field-flow fractionation. *Mar. Chem.* **118**, 119-
779 128.
780 Stolpe, B., Zhou, Z., Guo, L., and Shiller, A. M., 2014. Colloidal size distribution of humic- and
781 protein-like fluorescent organic matter in the northern Gulf of Mexico. *Mar. Chem.* **164**,
782 25-37, doi:10.1016/j.marchem.2014.05.007.
783 Wang, X., Cai, Y., and Guo, L., 2010. Preferential removal of dissolved carbohydrates during
784 estuarine mixing in the Bay of Saint Louis in the northern Gulf of Mexico. *Mar. Chem.*
785 **119**, 130-138.

Wang, X., Cai, Y., and Guo, L., 2013. Variations in abundance and size distribution of carbohydrates in the lower Mississippi River, Pearl River and Bay of St Louis. *Estuarine, Coastal and Shelf Science* **126**, 61-69.

Weishaar, J. L., Aiken, G. R., Bergamaschi, B. A., Fram, M. S., Fujii, R., and Mopper, K., 2003. Evaluation of specific ultraviolet absorbance as an indicator of the chemical composition and reactivity of dissolved organic carbon. *Environ. Sci. Technol.* **37**, 4702-4708, doi:10.1021/es030360x.

Wiener, J. G., Fremling, C. R., Korschgen, C. E., Kenow, K. P., Kirsch, E. M., Rogers, S. J., Yin, Y., and Sauer, J. S., 1996. Mississippi River, *Status and Trends of Nation's Biological Resources*. National Weahter Resouces Center, U.S. Geological Survey, Washington, D.C.

Williams, C. J., Yamashita, Y., Wilson, H. F., Jaffé, R., and Xenopoulos, M. A., 2010. Unraveling the role of land use and microbial activity in shaping dissolved organic matter characteristics in stream ecosystems. *Limnol. Oceanogr.* **55**, 1159-1171.

Williams, P. S., Xu, Y., Reschiglian, P., and Giddings, J. C., 1997. Colloid Characterization by Sedimentation Field-Flow Fractionation- Correction for Particle-Wall Interaction. *Anal. Chem.* **69**, 349-360.

Williams, S. K. R. and Keil, R. G., 1997. Monitoring the Biological and Physical Reactivity of Dextran Carbohydrates in Seawater Incubations Using Flow Field-Flow Fractionation. *J. Liq. Chromatogr. Relat. Technol.* **20**, 2815-2833.

Yamashita, Y. and Tanoue, E., 2003. Chemical characterization of protein-like fluorophores in DOM in relation to aromatic amino acids. *Mar. Chem.* **82**, 255-271.

Zanardi-Lamardo, E., Clark, C. D., Moore, C. A., and Zika, R. G., 2002. Comparison of the molecular mass and optical properties of colored dissolved organic material in two rivers and coastal waters by Flow Field-Flow Fractionation. *Environ. Sci. Technol.* **36**, 2806-2814.

Zhou, Z., Guo, L., Shiller, A. M., Lohrenz, S. E., Asper, V. L., and Osburn, C. L., 2013. Characterization of oil components from the Deepwater Horizon oil spill in the Gulf of Mexico using fluorescence EEM techniques. *Mar. Chem.* **148**, 10-21, doi:10.1016/j.marchem.2012.10.003.

Zhou, Z. and Guo, L. 2015. A critical evaluation of an asymmetrical flow field-flow fractionation system for colloidal size characterization of natural dissolved organic matter. *Journal of Chromatography A*., 1399, 53-64, doi:10.1016/j.chroma.2015.04.035.

821 Table 1

822 Hydrographic parameters and concentrations of dissolved organic carbon (DOC) and colloidal
823 organic carbon (COC) in samples from the lower Mississippi River (MR) and the East Pearl
824 River (PR).

| Sample ID | Sampling Date | Discharge ($m^3/s$) | Specific Conductivity (μS/cm) | Temp (˚C) | DOC (μM) | COC (μM) | COC/DOC (%) |
|---|---|---|---|---|---|---|---|
| MR | 23-Jan-09 | 16,622 | 382 | 6.3 | 256±1 | 151 | 59 |
| MR | 20-Feb-09 | 14,926 | 343 | 8.8 | 236±2 | - | - |
| MR | 27-Mar-09 | 18,774 | 314 | 13 | 324±2 | 183 | 57 |
| MR | 24-Apr-09 | 21,345 | 350 | 15.9 | 296±2 | - | - |
| MR | 29-May-09 | 34,688 | 308 | 36.7 | 339±2 | 204 | 60 |
| MR | 29-Jun-09 | 19,658 | 326 | 29.8 | 317±2 | - | - |
| MR | 30-Jul-09 | 10,395 | 388 | 27.8 | 270±2 | - | - |
| MR | 26-Aug-09 | 9,047 | 391 | 28.8 | 264±2 | - | - |
| MR | 29-Sep-09 | 11,771 | 330 | 25.6 | 299±4 | 182 | 61 |
| MR | 29-Oct-09 | 20,445 | 276 | 16.1 | 343±2 | - | - |
| MR | 30-Nov-09 | 20,048 | 324 | 13 | 337±2 | - | - |
| MR | 31-Dec-09 | 22,283 | 267 | 7 | 265±1 | - | - |
| MR | 28-Jan-10 | 17,695 | 355 | 7.3 | 275±1 | 167 | 61 |
| MR | 25-Feb-10 | 25,482 | 290 | 5.7 | 237±1 | - | - |
| PR | 15-Jan-09 | 1189 | 48 | 10.3 | 728±2 | - | - |
| PR | 13-Feb-09 | 127 | - | 16 | 376±1 | - | - |
| PR | 14-Mar-09 | 96 | 78 | 21.7 | 326±1 | - | - |
| PR | 2-Apr-09 | 2,011 | 37 | 18.8 | 1121±5 | - | - |
| PR | 7-Apr-09 | 1,470 | 39 | 17.5 | 834±3 | 604 | 72 |
| PR | 2-May-09 | 116 | 75 | 27.4 | 438±2 | - | - |
| PR | 22-May-09 | 289 | 60 | 24.9 | 666±3 | - | - |
| PR | 23-Jun-09 | 66 | 238 | 32.8 | 398±3 | - | - |
| PR | 15-Jul-09 | 56 | 2,500 | 31 | 353±2 | - | - |
| PR | 17-Aug-09 | 65 | 4,470 | 30.4 | 617±3 | - | - |
| PR | 23-Sep-09 | 94 | 266 | 28.3 | 899±2 | - | - |
| PR | 26-Oct-09 | 881 | 80 | 17.7 | 889±2 | - | - |
| PR | 25-Nov-09 | 114 | 83 | 18.2 | 569±1 | - | - |
| PR | 28-Dec-09 | 943 | 39 | 9.8 | 790±2 | - | - |
| PR | 31-Jan-10 | 983 | 48 | 10.5 | 736±2 | - | - |
| PR | 25-Feb-10 | 428 | 38 | 11.3 | 579±2 | - | - |

825
826

827 Table 2

828 Salinity and concentrations of DOC and COC in end-member water samples used for laboratory
829 mixing experiments and in samples from the St. Louis Bay (SLB), Jourdan River (JR), and
830 Mississippi Sound (MS), and Mississippi Bight (MB).

| Sample ID | Sampling Date | Latitude (°N) | Longitude (°W) | Salinity | DOC (μM) | COC (μM) | COC/DOC (%) |
|---|---|---|---|---|---|---|---|
| JR | Oct 06 2009 | 30°23′12″ | 89°27′46″ | 0.1 | 1618±4 | 1107 | 68 |
| SLB 1 | Oct 15 2009 | 30°20′35″ | 89°19′10″ | 4.9 | 1176±5 | 665 | 57 |
| SLB 2 | Oct 15 2009 | 30°17′58″ | 89°18′2″ | 9.8 | 752±3 | 390 | 52 |
| SLB 3 | Oct 15 2009 | 30°16′42″ | 89°17′30″ | 14.5 | 421±1 | 189 | 45 |
| MS | Oct 15 2009 | 30°11′53″ | 89°10′50" | 18 | 390±3 | 167 | 43 |
| MB | Oct 15 2009 | 30°9′37" | 89°2′45" | 26 | 234±2 | 99 | 45 |
| JR | Jan 13 2010 | 30°23′12″ | 89°27′46″ | 0.1 | 387±3 | - | - |
| MB | Jan 13 2010 | 30°2'35" | 88°39'02" | 30 | 154±1 | - | - |

831
832

833 Table 3

834 Instrument parameters for the analysis using flow field-flow fractionation.

| Parameter | Details or values |
|---|---|
| Accumulation wall membrane | 1 kDa polyether sulfone (Omega, Pall Filtron) |
| Carrier solution | 10 mM NaCl, 5 mM boric acid, pH = 8 |
| Sample volume (ml) | 10 |
| *On-line pre-concentration:* | |
| Channel flow rate (ml/min) | 0.5 |
| Focus flow rate (ml/min) | 4.5 |
| Focus (injection) time (min) | 10 |
| *Relaxation:* | |
| Equilibration time (min) | 1 |
| *Elution:* | |
| Channel flow rate (ml/min) | 0.5 |
| Cross flow rate (ml/min) | 3.0 |
| Run time (min) | 60 |

835
836

837 Figure captions
838
839 Fig. 1. Sampling locations in the lower Mississippi River (MR) at Baton Rouge, Louisiana; the
840 East Pearl River (EPR) near Stennis Space Center, Mississippi; the Jourdan River (JR); and St.
841 Louis Bay (SLB), the Mississippi Sound (MS), and Mississippi Bight (MB) in the northern Gulf
842 of Mexico.
843
844 Fig. 2. Examples of colloidal size spectra of chromophoric ($UV_{254}$), humic-like ($Fluo_{350/450}$), and
845 protein-like ($Fluo_{275/340}$) DOM in the lower Mississippi River (sample collected on November 30,
846 2009), the East Pearl River (December 28, 2009), the Jourdan River (Oct 15, 2009), St. Louis
847 Bay (SLB) (Oct 15, 2009, S=15), and Mississippi Bight (S=30). The peak observed at >20 nm
848 corresponds to all materials larger than 20 nm that eluted together after shutting down of cross
849 flow.
850
851 Fig. 3. Relative importance of colloidal chromophoric (top panel), humic-like (middle panel) and
852 protein-like (bottom panel) DOM in the 0.5-4 nm, 4-20 nm and >20 nm size fractions, as
853 compared with the total FlFFF-recoverable colloidal fraction, in the lower Mississippi River and
854 the East Pearl River.
855
856 Fig. 4. Variations of DOC (upper panels) and UV-absorbance at 254 nm, $a_{254}$ (lower panels)
857 along the river-sea water transect in field samples (left panels) and samples from the laboratory
858 mixing experiment (right panels). Note that in the plots for the field samples, dotted lines were
859 marked at salinity = 15, corresponding to the salinity at the mouth of St. Louis Bay, to help
860 visualize different DOM characteristics inside and outside the Bay.
861
862 Fig. 5. Variations of $[UV_{254}]_{FFF}$ (ppb-QSE), $[Fluo_{350/450}]_{FFF}$ (ppb-QSE), $[Fluo_{275/340}]_{FFF}$ (ppb-
863 QSE), and $[Fluo_{275/340}]_{FFF}/[Fluo_{350/450}]_{FFF}$ ratio along the river-sea water transect in the St. Louis
864 Bay estuary (left panels) and in samples from the laboratory mixing experiment (right panels).
865 Again, the dotted lines at S=15 in the plots for field samples help visualize different colloidal
866 DOM mixing behavior inside and outside the bay.
867

868 Fig. 6. Relative importance of colloidal humic-like ($Fluo_{350/450}$, left panel) and protein-like
869 ($Fluo_{275/340}$, right panel) DOM in the 0.5-4 nm, 4-20 nm and >20 nm size fractions, as calculated
870 by their fractions in the FlFFF-recoverable colloidal size range, from the Jourdan River (JR), St.
871 Louis Bay (SLB) estuary, and the Mississippi Bight (MB).
872
873 Fig. 7. Variations of $[UV_{254}]_{0.5\text{-}4nm}$ (ppb-QSE) and $[Fluo_{350/450}]_{0.5\text{-}4nm}$ (ppb-QSE) along the salinity
874 gradient in field samples (left panels) and in the laboratory mixing experiment (right panels). The
875 dotted lines at S =15 were also added.
876
877 Fig. 8. Change in colloidal size spectra of protein-like DOM ($Fluo_{275/340}$) during the estuarine
878 mixing experiment using end-member river water and seawater. A total of six examples are
879 shown in the order of increasing salinity.
880
881 Fig. 9. Variations of colloidal protein-like DOM in the small size ($[Fluo_{275/340}]_{0.5\text{-}4nm}$ (ppb-QSE),
882 upper panel), mid size ($[Fluo_{275/340}]_{4\text{-}8nm}$ (ppb-QSE), middle panel), and large size fraction
883 ($[Fluo_{275/340}]_{>20nm}$ (ppb-QSE), lower panel) during the laboratory mixing experiment.
884
885 Fig. 10. Comparisons of the ratio of mid- to small sized colloidal protein-like DOM
886 ($[Fluo_{275/340}]_{4\text{-}8nm}/[Fluo_{275/340}]_{0.5\text{-}4nm}$, upper panels) and the ratio of large to small sized protein-
887 like DOM ($[Fluo_{275/340}]_{>20nm}/[Fluo_{275/340}]_{0.5\text{-}4nm}$, lower panels) between field data (left panels) and
888 laboratory mixing experiment (right panels). The dotted lines at S = 15 were also marked.

Fig. 1

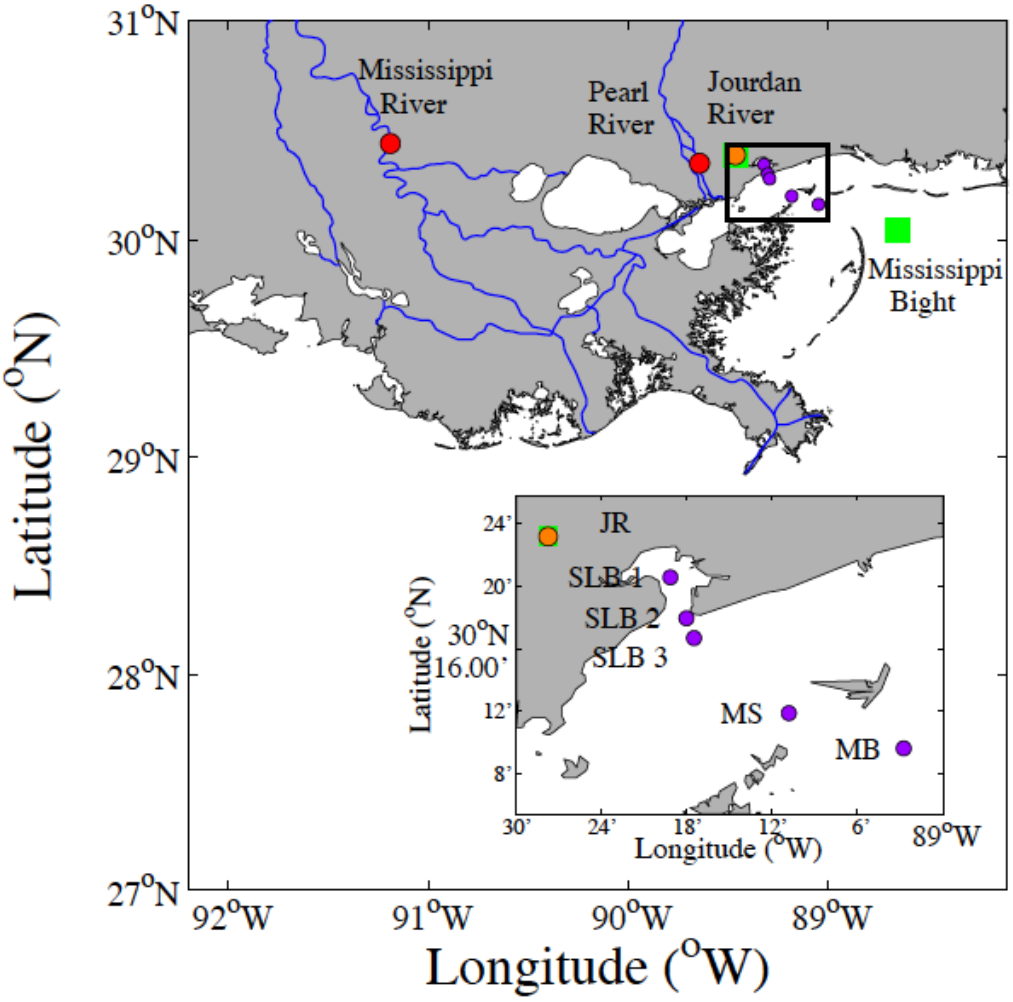
31°N
30°N
29°N
28°N
27°N
92°W
91°W
90°W
89°W
Latitude (°N)
Longitude (°W)
Mississippi River
Pearl River
Jourdan River
Mississippi Bight
JR
SLB 1
SLB 2
SLB 3
MS
MB
24'
20'
30°N 16.00'
12'
8'
30'
24'
18'
12'
6'
89°W
Latitude (°N)
Longitude (°W)

Fig. 2

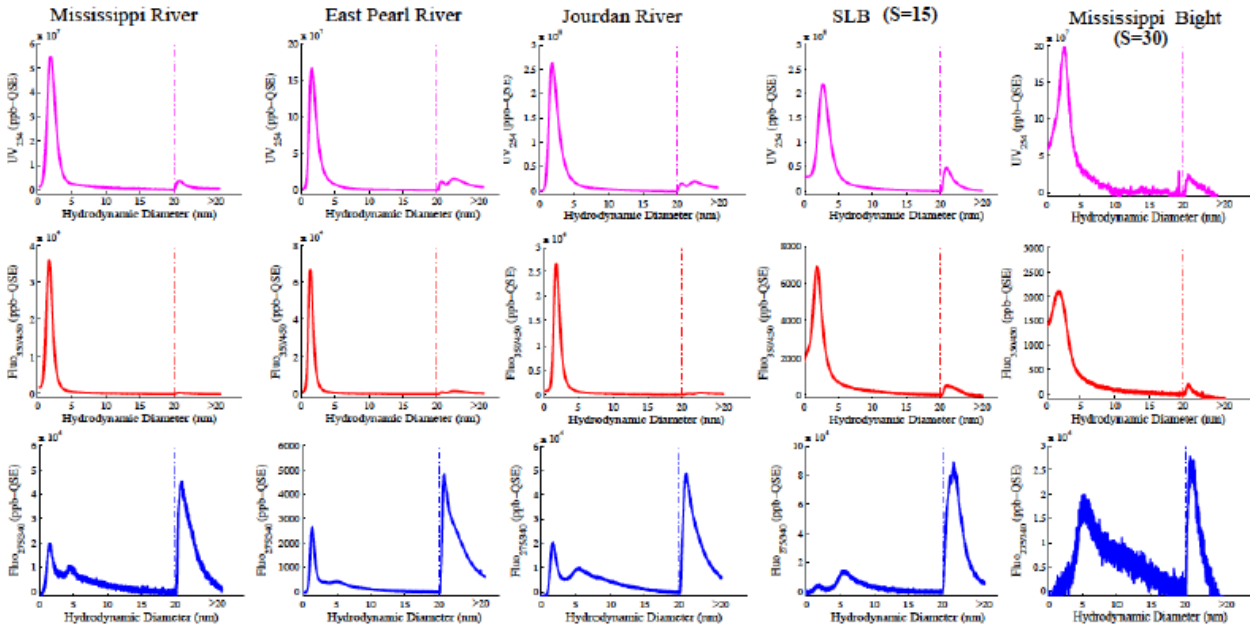
Mississippi River
East Pearl River
Jourdan River
SLB (S=15)
Mississippi Bight (S=30)
Hydrodynamic Diameter (nm)

Fig. 3

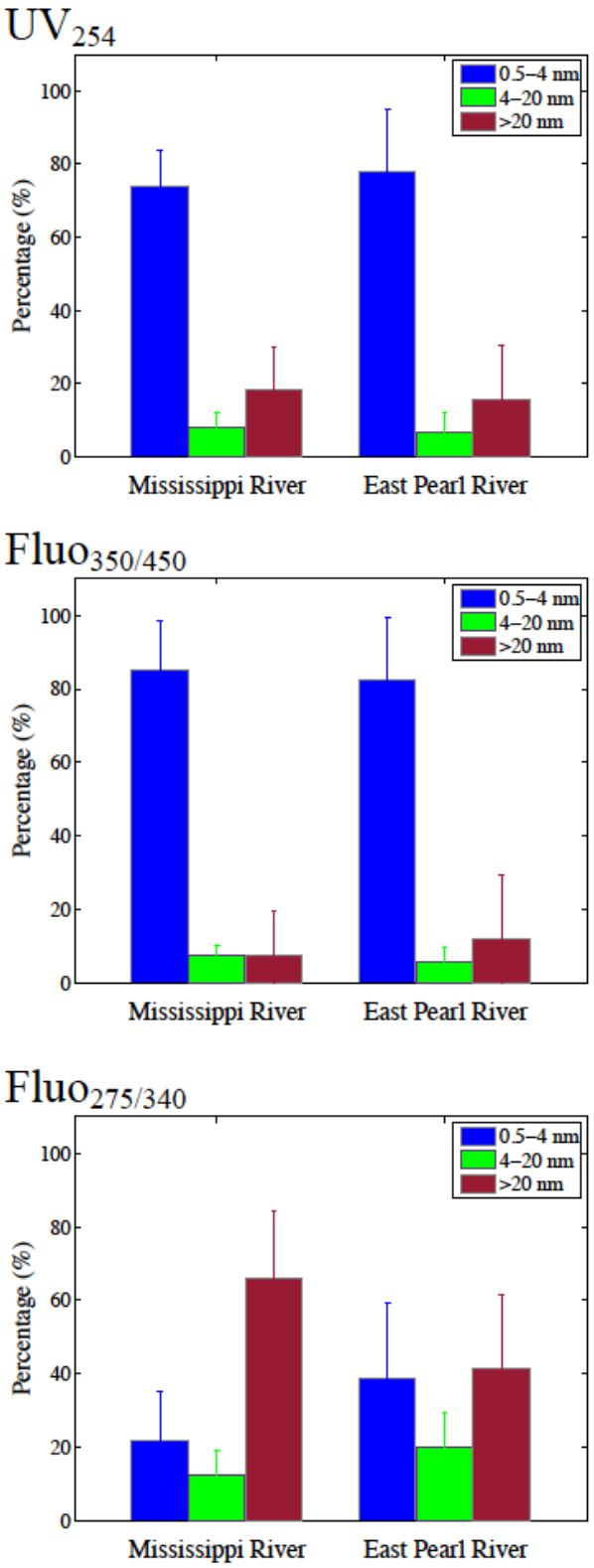
UV254
0.5–4 nm
4–20 nm
>20 nm
Percentage (%)
0
20
40
60
80
100
Mississippi River
East Pearl River
Fluo350/450
0.5–4 nm
4–20 nm
>20 nm
Percentage (%)
0
20
40
60
80
100
Mississippi River
East Pearl River
Fluo275/340
0.5–4 nm
4–20 nm
>20 nm
Percentage (%)
0
20
40
60
80
100
Mississippi River
East Pearl River

Fig. 4

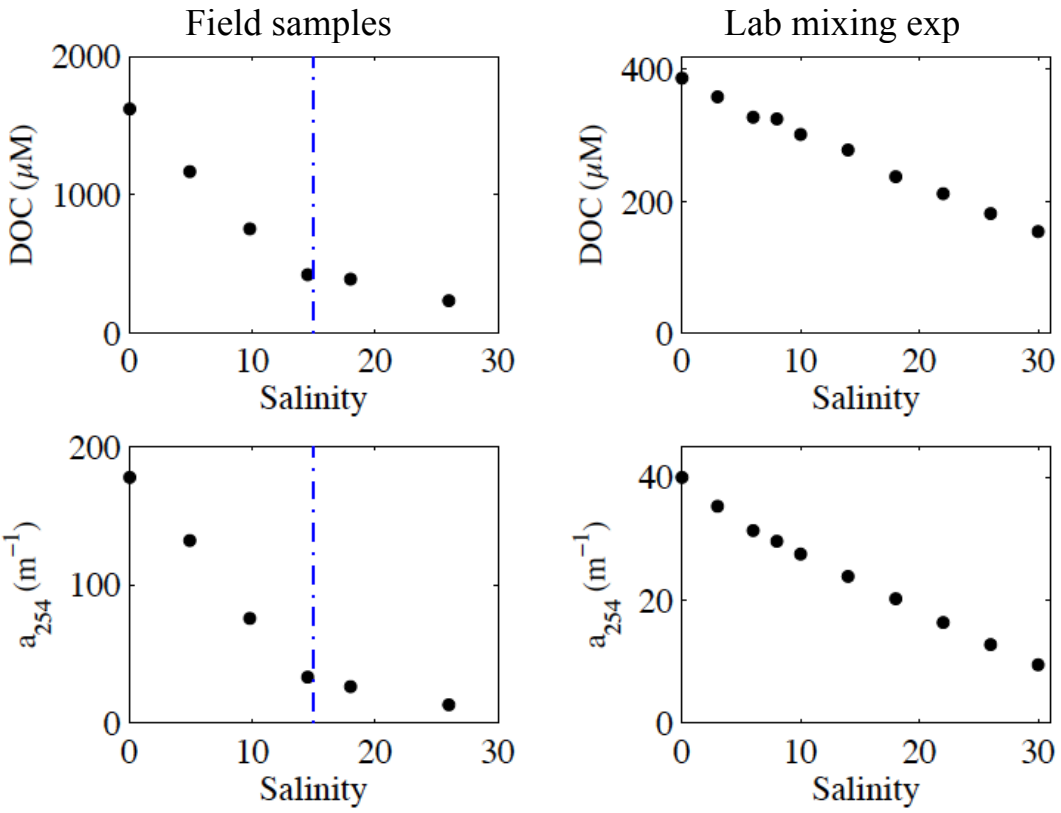
Field samples
Lab mixing exp
DOC (μM)
2000
1000
0
400
200
0
10
20
30
Salinity
$a_{254}$ ($m^{-1}$)
200
100
40
20

Fig. 5

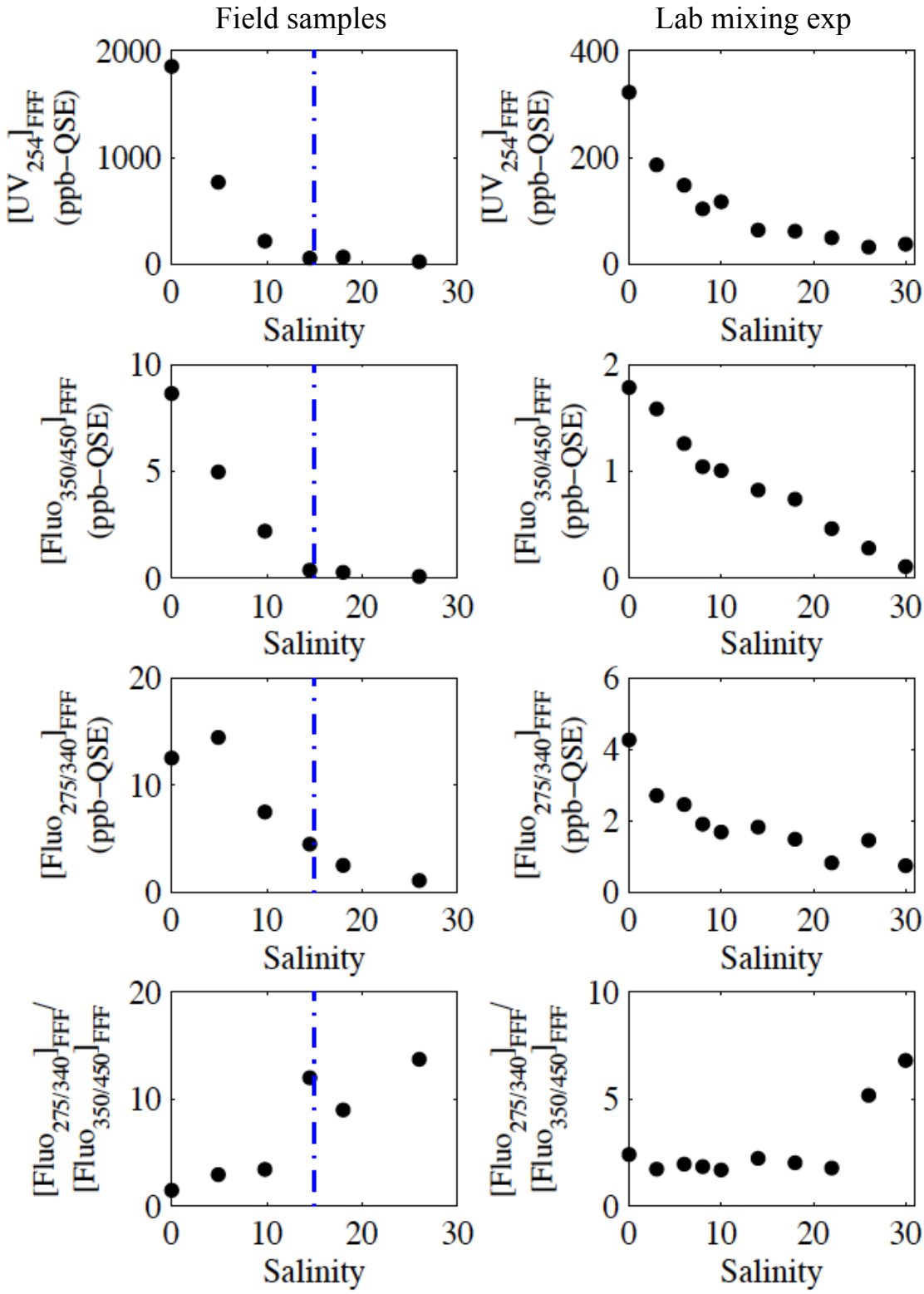
Field samples
Lab mixing exp
[UV254]FFF (ppb–QSE)
[Fluo350/450]FFF (ppb–QSE)
[Fluo275/340]FFF (ppb–QSE)
[Fluo275/340]FFF / [Fluo350/450]FFF
Salinity
0
10
20
30
2000
1000
400
200
5
2
1
6
4

Fig. 6

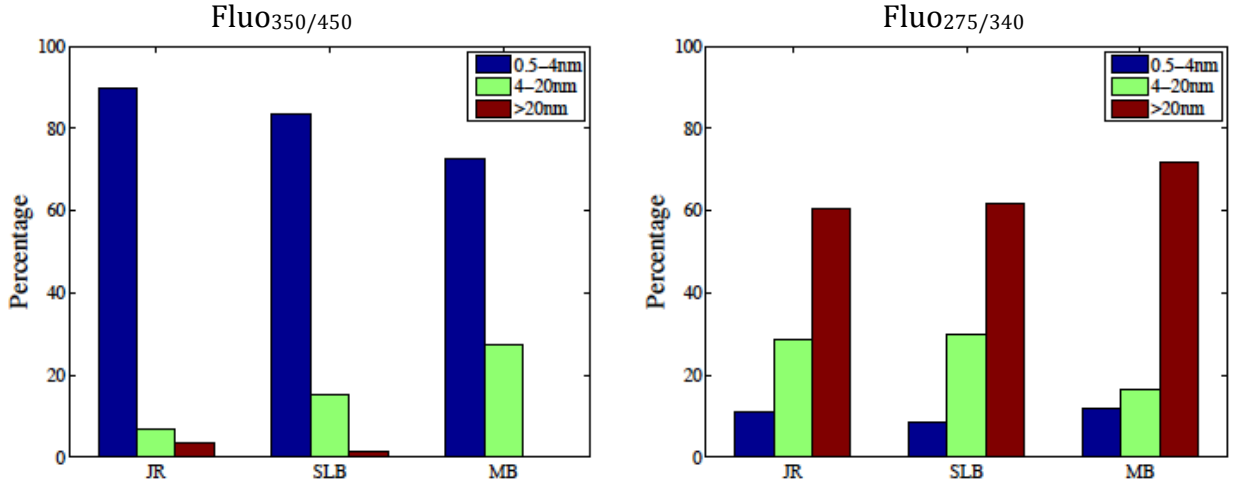
Fluo350/450
Percentage
100
80
60
40
20
0
JR
SLB
MB
0.5–4nm
4–20nm
>20nm
Fluo275/340
Percentage
100
80
60
40
20
0
JR
SLB
MB
0.5–4nm
4–20nm
>20nm

Fig. 7

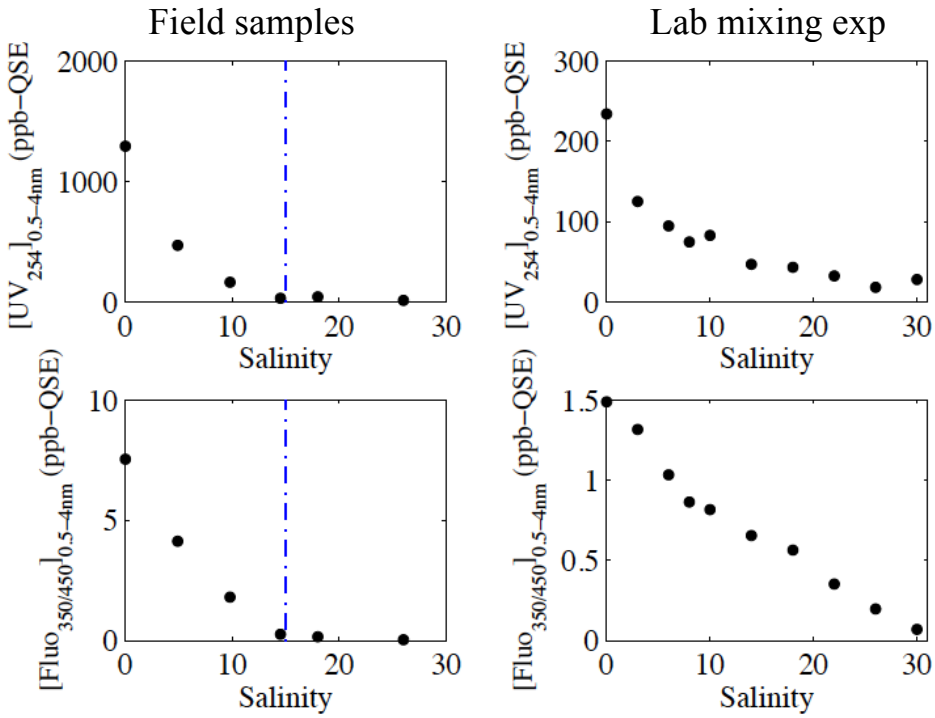
Field samples
Lab mixing exp
[UV254]0.5–4nm (ppb–QSE)
[Fluo350/450]0.5–4nm (ppb–QSE)
Salinity
0
10
20
30
2000
1000
300
200
100
1.5
1
0.5
5

Fig. 8

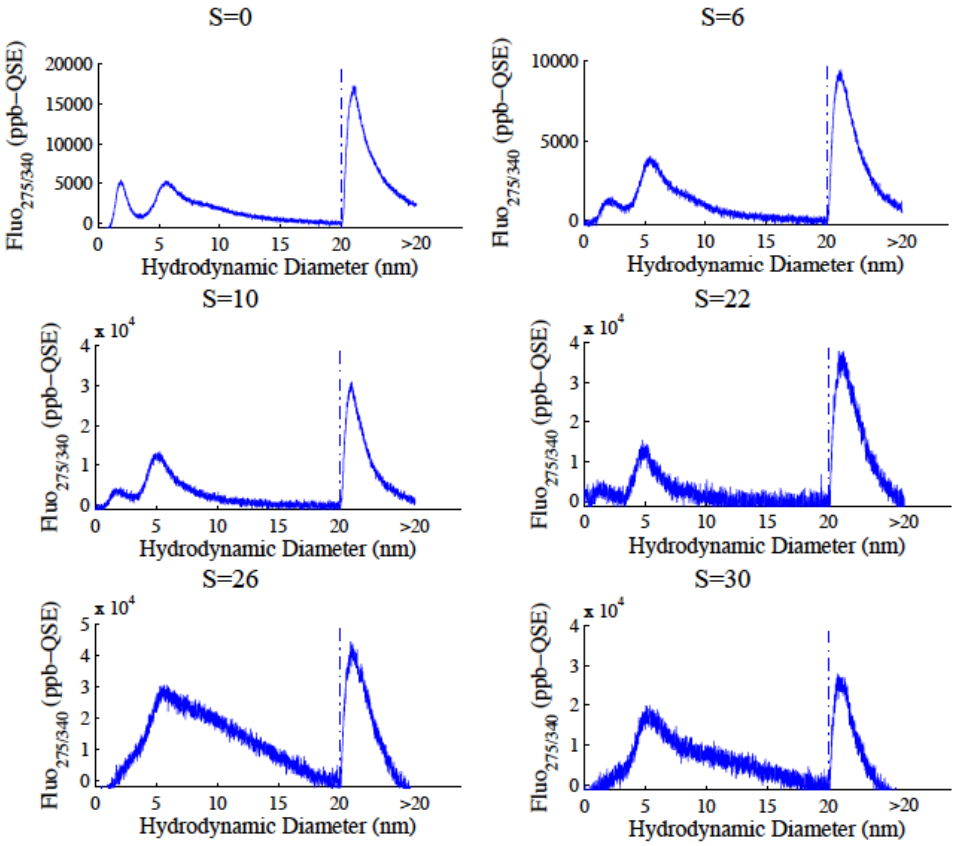
S=0
S=6
S=10
S=22
S=26
S=30
Fluo275/340 (ppb–QSE)
Hydrodynamic Diameter (nm)
0
5
10
15
20
>20
x 10^4

Fig. 9

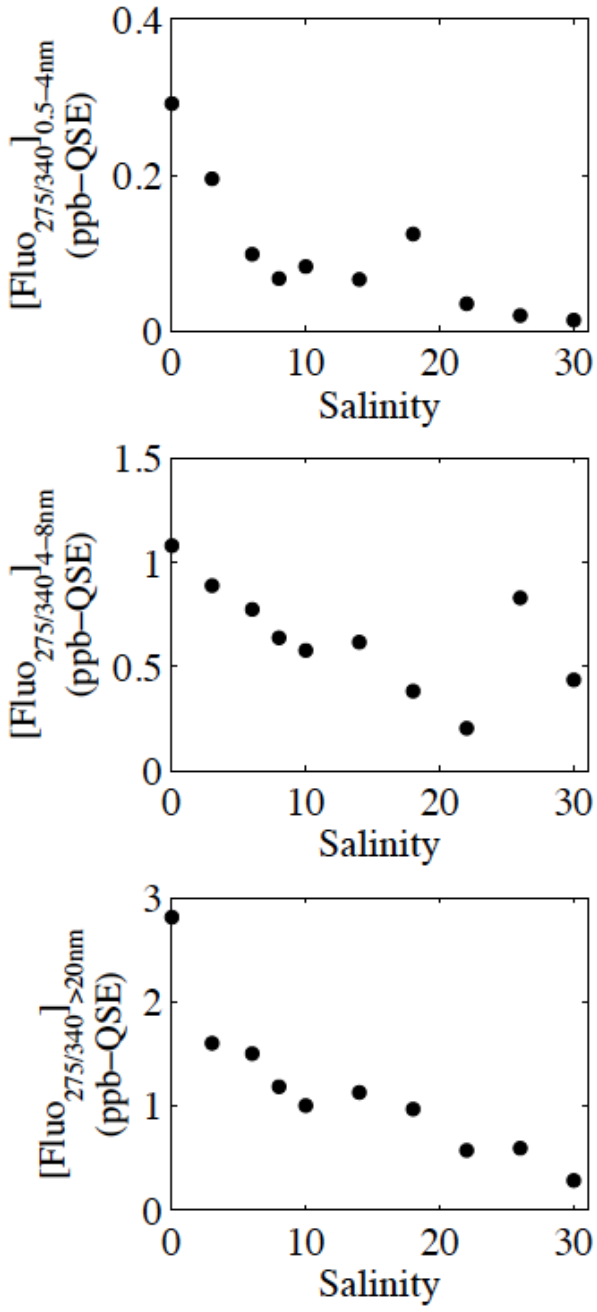
[Fluo275/340]0.5–4nm (ppb–QSE)
0.4
0.2
0
0
10
20
30
Salinity
[Fluo275/340]4–8nm (ppb–QSE)
1.5
1
0.5
0
0
10
20
30
Salinity
[Fluo275/340]>20nm (ppb–QSE)
3
2
1
0
0
10
20
30
Salinity

Fig. 10

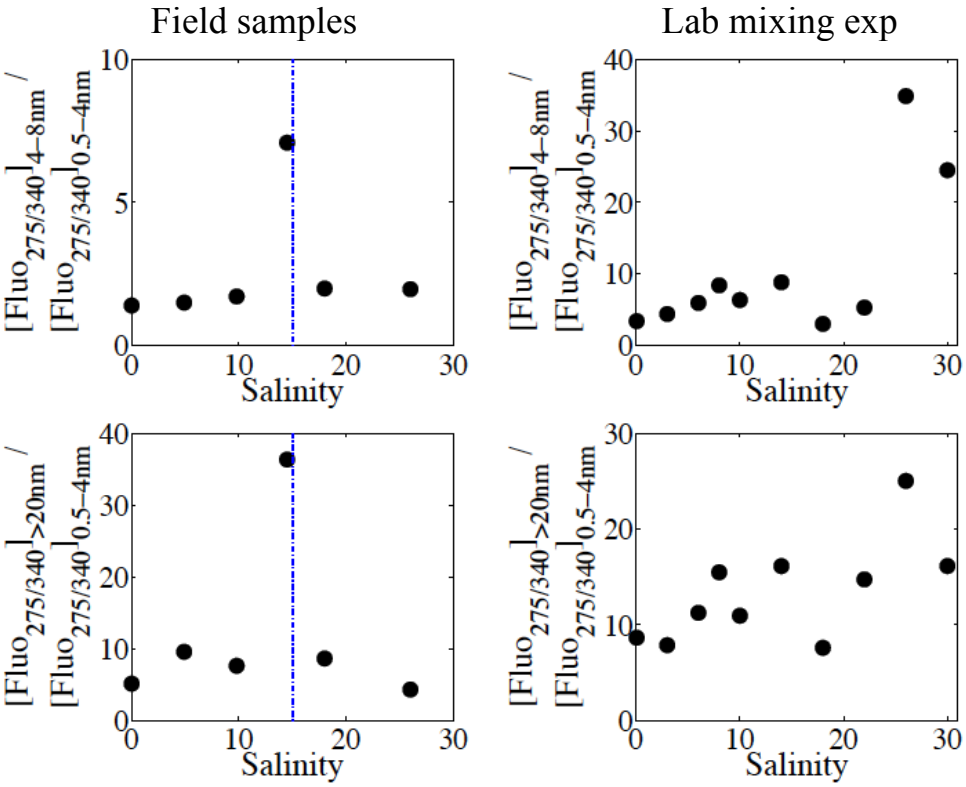
Field samples
Lab mixing exp
[Fluo275/340]4–8nm / [Fluo275/340]0.5–4nm
[Fluo275/340]>20nm / [Fluo275/340]0.5–4nm
Salinity
0
5
10
20
30
40